

**CO₂ Corrosion Study of Carbon Steel in Natural and Induced Film Forming
Environment**

by

Ameirul Azraie Bin Mustadza

Dissertation submitted in partial fulfilment of
the requirements for the
Bachelor of Engineering (Hons)
(Mechanical Engineering)

JANUARY 2009

Universiti Teknologi PETRONAS
Bandar Seri Iskandar
31750 Tronoh
Perak Darul Ridzuan

CERTIFICATION OF APPROVAL

CO₂ Corrosion Study of Carbon Steel in Natural and Induced Film Forming Environment

by

Ameirul Azraie Bin Mustadza

A project dissertation submitted to the
Mechanical Engineering Programme
Universiti Teknologi PETRONAS
in partial fulfilment of the requirement for the
BACHELOR OF ENGINEERING (Hons)
(MECHANICAL ENGINEERING)

Approved by,

Assoc. Prof. Ir. Dr. Mokhtar Che Ismail

UNIVERSITI TEKNOLOGI PETRONAS

TRONOH, PERAK

January 2009

CERTIFICATION OF ORIGINALITY

This is to certify that I am responsible for the work submitted in this project, that the original work is my own except as specified in the references and acknowledgements, and that the original work contained herein have not been undertaken or done by unspecified sources or persons.

AMEIRUL AZRAIE BIN MUSTADZA

ABSTRACT

Carbon dioxide (CO₂) corrosion prediction is complicated as it affects the application of carbon steel material due to possibility of high corrosion rate and the formation of protective iron carbonate (FeCO₃) film layers. The formation of FeCO₃ film layers is observed to reduce corrosion rate particularly at high temperature and high pH. Most of the FeCO₃ film formation studies were done by inducing film formation through the addition of Fe²⁺ ions into the test solution to reach saturation condition where the product of Fe²⁺ and CO₃²⁻ exceeds the solubility product limit and not in natural film condition. This project aims to understand the FeCO₃ film formation by conducting laboratory experiment of CO₂ corrosion on carbon steel in natural and induced film forming environment with Fe²⁺ concentration ($c_{\text{Fe}^{2+}}$) of 50 ppm. The study is conducted at various temperatures from 25°C to 80°C at pH 6.0, partial pressure of CO₂ at 1 bar and stagnant conditions to observe how these parameters affect the CO₂ corrosion rate and formation of FeCO₃ film layers. Two electrochemical test techniques namely Electrochemical Impedance Spectroscopy (EIS) and Linear Polarization Resistance (LPR) are used. EIS technique shows that as the temperature increases the average corrosion rate increases while for LPR technique, the average corrosion rate increases at temperature of 25°C until 60°C before decreases at temperature of 80°C with lower average corrosion rate in induced film forming environment. It is observed that the average corrosion rate is relatively lower in induced film forming environment since the increase of Fe²⁺ concentration results in faster formation of FeCO₃ film layers. Based on the results of the corrosion tests in both conditions, it shows that for corrosion prediction work, the test is best represented by natural film forming environment. Induced film condition is only suitable for the study in relations to film initiation, growth and propagation.

ACKNOWLEDGEMENTS

First and foremost, the author would like to thank Allah, the Most Gracious and the Most Merciful for His blessings throughout the process of completing this project. The author would also like to thank his supervisor, Assoc. Prof. Ir. Dr. Mokhtar Che Ismail, for the tremendous support, advice, guidance and encouragement throughout this project and in the preparation of this report. The author wishes to convey his heartfelt thanks to the following postgraduate students; Ms. Anis Amilah Ab Rahman, Mr. Budi Agung Kurniawan, and Mr. Yuli Panca Asmara who have also contributed significantly with their priceless invaluable and mentoring from time to time in this project. The author wishes special thanks to the Mechanical Laboratory Technicians particularly Mr. M Faisal Ismail for his help and assistance during sample preparation and Mr. Irwan Othman in using the SEM. The author is also very grateful to his fellow friends; Mr. Adzlan Ayob and Ms. Wan Normimi Roslini Abdullah for their advice and opinion on this project. Not forgetting, a word of thanks also goes to the author's beloved parents, Mr. Mustadza Md. Yusop and Madam Noorfah Senusi for their support and encouragement which has indeed inspired the author to complete this project. Lastly, the author would like to thank all those people who have contributed in one way or another, directly or indirectly in the process of carrying out this project.

TABLE OF CONTENTS

CERTIFICATION OF APPROVAL	i
CERIFICATION OF ORIGINALITY	ii
ABSTRACT	iii
ACKNOWLEDGEMENTS	iv
LIST OF FIGURES	vii
LIST OF TABLES	x
CHAPTER 1:	INTRODUCTION	.	.	.	1
	1.1	Background of Study	.	.	1
	1.2	Problem Statement	.	.	2
	1.3	Objectives	.	.	2
	1.4	Scope of Study	.	.	3
	1.5	Relevancy of the Project	.	.	3
	1.6	Feasibility of the Project	.	.	3
CHAPTER 2:	LITERATURE REVIEW	.	.	.	4
	2.1	Overview of Carbon Dioxide Corrosion			5
	2.2	Iron Carbonate Film Formation	.		9
	2.3	Electrochemical Measurement Techniques			12
CHAPTER 3:	METHODOLOGY	.	.	.	22
	3.1	Research Methodology	.	.	22
	3.2	Electrochemical Measurement Techniques			23

	3.3	Materials	24
	3.4	Sample Preparation	24
	3.5	Test Environment	25
	3.6	Experimental Setup	26
	3.7	Experimental Procedure	27
CHAPTER 4:		RESULTS AND DISCUSSION	29
	4.1	Natural Film Forming Environment	29
	4.2	Induced Film Forming Environment	36
	4.3	Overall Corrosion Rate	44
CHAPTER 5:		CONCLUSION AND RECOMMENDATIONS	46
	5.1	Conclusion	46
	5.2	Recommendations	47
REFERENCES			49
APPENDIX:		METHOD OF Fe²⁺ ADDITION	51

LIST OF FIGURES

Figure 2.1: Sinusoidal AC voltage and current signals	13
Figure 2.2: Relationship between sinusoidal AC current and rotating vector representation	14
Figure 2.3: In-phase and out-of-phase rotation of current and voltage vectors	15
Figure 2.4: Impedance vector	15
Figure 2.5: Nyquist plot	17
Figure 2.6: Impedance vs. frequency	17
Figure 2.7: Phase angle vs. frequency	17
Figure 2.8: Circuit that models simple impedance response	19
Figure 2.9: Circuit that models impedance in the presence of diffusion	20
Figure 3.1: Project flow chart	22
Figure 3.2: The working electrode	25
Figure 3.3: The exposed area	25
Figure 3.4: Sample cold mounting	25
Figure 3.5: Metallurgical grinder	25

Figure 3.6: Experimental setup	26
Figure 4.1: Impedance spectra, presented as a Nyquist plot, recorded for 24 hours immersion of a carbon steel specimen in CO ₂ saturated 3% NaCl solution at various temperatures	29
Figure 4.2: Impedance spectra, presented as a Nyquist plot, recorded for 24 hours immersion of a carbon steel specimen in CO ₂ saturated 3% NaCl solution at temperature of 80°C	30
Figure 4.3: Average corrosion rate at pH 6 of a carbon steel specimen in CO ₂ saturated 3% NaCl solution at various temperatures	31
Figure 4.4: Impedance spectra, presented as a Bode plot of phase angle against frequency, recorded for 24 hours immersion of a carbon steel specimen in CO ₂ saturated 3% NaCl solution at various temperatures	32
Figure 4.5: Equivalent circuits used to represent the impedance results at (a) temperature of 25°C, 40°C, and 60°C; (b) temperature of 80°C	32
Figure 4.6: Corrosion rate at pH 6, recorded for 24 hours immersion of a carbon steel specimen in CO ₂ saturated 3% NaCl solution at various temperatures	33
Figure 4.7: Average corrosion rate at pH 6 of a carbon steel specimen in CO ₂ saturated 3% NaCl solution at various temperatures	34
Figure 4.8: SEM images, for 24 hours immersion of a carbon steel specimen in CO ₂ saturated 3% NaCl solution at temperature of 80°C (a) 300x (b) 1000x (c) 3000x	36

Figure 4.9: Impedance spectra, presented as a Nyquist plot, recorded for 24 hours immersion of a carbon steel specimen in CO₂ saturated 3% NaCl solution with an addition of 50 ppm concentration of ions Fe²⁺ at various temperatures . 37

Figure 4.10: Impedance spectra, presented as a Nyquist plot, recorded for 24 hours immersion of a carbon steel specimen in CO₂ saturated 3% NaCl solution with an addition of 50 ppm concentration of ions Fe²⁺ at temperature of 80°C . 38

Figure 4.11: Average corrosion rate at pH 6 of a carbon steel specimen in CO₂ saturated 3% NaCl solution with an addition of 50 ppm concentration of ions Fe²⁺ at various temperatures 38

Figure 4.12: Impedance spectra, presented as a Bode plot of phase angle against frequency, recorded for 24 hours immersion of a carbon steel specimen in CO₂ saturated 3% NaCl solution with an addition of 50 ppm concentration of ions Fe²⁺ at various temperatures 39

Figure 4.13: Corrosion rate at pH 6, recorded for 24 hours immersion of a carbon steel specimen in CO₂ saturated 3% NaCl solution with an addition of 50 ppm concentration of ions Fe²⁺ at various temperatures 40

Figure 4.14: Average corrosion rate at pH 6 of a carbon steel specimen in CO₂ saturated 3% NaCl solution with an addition of 50 ppm concentration of ions Fe²⁺ at various temperatures 41

Figure 4.15: SEM images for 24 hours immersion of a carbon steel specimen in CO₂ saturated 3% NaCl solution with an addition of 50 ppm concentration of ions Fe²⁺ at temperature of 80°C (a) 300x (b) 1000x (c) 3000x 43

LIST OF TABLES

Table 2.1: Circuit elements	16
Table 3.1: Chemical composition of BS 970	24
Table 3.2: Test matrix for the research	27
Table 4.1: Average corrosion rate for natural film forming environment and induced film forming environment	44

CHAPTER 1

INTRODUCTION

1.1 Background of Study

In oil and gas industry, CO₂ corrosion has been a recognized problem in production and transportation facilities for many years. This result from the fact that an aqueous phase is normally associated with the oil and gas production systems which promote an electrochemical reaction between carbon steel and the contacting aqueous phase. CO₂ is extremely soluble in water but has a greater solubility in hydrocarbon fluids produced in the oil and gas production systems and, although it does not cause the catastrophic failure mode of cracking associated with H₂S; its presence can nevertheless result in very high corrosion rate particularly where the mode of attack on carbon steel is localized [1].

Nevertheless, the formation of FeCO₃ film layers as the product of CO₂ corrosion reaction somehow helps to reduce corrosion rate provided that FeCO₃ film layers are stable and protective. The study of CO₂ corrosion rate and FeCO₃ film formation been carried out rapidly in the last 30 years to develop the understanding and modeling the kinetics of FeCO₃ precipitation process as they are dependent on the environmental effects such as temperature, pH, CO₂ partial pressure, Fe²⁺ concentration and flow velocity.

However, most of the FeCO₃ film formation studies were done by inducing film formation through the addition of Fe²⁺ ions into the test solution. These studies are not simulating the natural film forming environment in the field operations. The results based on induced film formation is not accurate because the increase of Fe²⁺ ions in the

solution will accelerate the precipitation rate thus help to reduce the corrosion rate significantly which is not the case in natural film forming environment.

1.2 Problem Statement

The CO₂ corrosion rate and formation of protective FeCO₃ film layers are affected by several parameters such as temperature, pH, CO₂ partial pressure, Fe²⁺ concentration and flow velocity. However, a full description of how these parameters affect the CO₂ corrosion rate and formation of protective FeCO₃ film layers is far too complicated yet it is still possible to predict the CO₂ corrosion rate under specific conditions. This project aims to understand the FeCO₃ film formation by conducting laboratory experiment of CO₂ corrosion on carbon steel in natural and induced film forming environment with Fe²⁺ concentration ($c_{\text{Fe}^{2+}}$) of 50 ppm. The study is conducted at various temperatures (t), from 25°C to 80°C to observe how these parameters affect the CO₂ corrosion rate and formation of FeCO₃ film layers. The other parameters include pH 6.0, partial pressure of CO₂ at 1 bar and stagnant conditions. The analysis will be done using EIS, LPR and SEM to determine the CO₂ corrosion rate, film type and its protectiveness to CO₂ corrosion.

1.3 Objectives

The objectives of this project are:

- To understand the FeCO₃ film formation in natural and induced film forming environment through corrosion rate measurement and surface morphology analysis.
- To compare the effect of temperature on the corrosion rate of carbon steel in natural and induced film forming environment.

1.4 Scope of Study

The scope of this project is:

- To study and analyze the effect of FeCO_3 film formation on CO_2 corrosion rate using EIS, LPR and SEM in natural and induced film forming environment with Fe^{2+} concentration ($c_{\text{Fe}^{2+}}$) of 50 ppm. The study is conducted at various temperatures (t) of 25°C, 40°C, 60°C and 80°C. The other parameters include pH 6.0, partial pressure of CO_2 at 1 bar and stagnant conditions.

1.5 Relevancy of the Project

The study of the effect of FeCO_3 film formation on CO_2 corrosion rate using EIS, LPR and SEM in natural and induced film forming environment is very important in the oil and gas industry. It is because the results obtained from the laboratory experiments will help to provide a better understanding on the FeCO_3 film formation in natural and induced film forming environment, thus, help to provide a reliable prediction of CO_2 corrosion rate which leads to cost-effective and safe design of production and transportation facilities used in the oil and gas industry.

1.6 Feasibility of the Project

The project was started by collecting reading materials such as books, journals and technical papers specifically on CO_2 corrosion of carbon steel, formation of protective FeCO_3 film layers and corrosion measurement technique. Research was done continuously throughout this project to get a better understanding on this project. The project was then focused on conducting laboratory experiments on carbon steel in CO_2 environment whereby analysis were carried out using EIS, LPR and SEM to determine the CO_2 corrosion rate, film type and its protectiveness to CO_2 corrosion.

CHAPTER 2

LITERATURE REVIEW

In oil and gas industry, CO₂ corrosion has been a recognized problem in production and transportation facilities for many years. It is a major source of concern in the application of carbon steel. This result from the fact that an aqueous phase is normally associated with the oil and gas production systems which promote an electrochemical reaction between carbon steel and the contacting aqueous phase. CO₂ is extremely soluble in water but has a greater solubility in hydrocarbon fluids produced in the oil and gas production systems and, although it does not cause the catastrophic failure mode of cracking associated with H₂S; its presence can nevertheless result in very high corrosion rate particularly where the mode of attack on carbon steel is localized [1].

Nevertheless, the formation of FeCO₃ film layers as the product of CO₂ corrosion reaction somehow helps to reduce corrosion rate provided that FeCO₃ film layers are stable and protective. The study of CO₂ corrosion rate and FeCO₃ film formation been carried out rapidly in the last 30 years to develop the understanding and modeling the kinetics of FeCO₃ precipitation process as they are dependent on the environmental effects such as temperature, pH, CO₂ partial pressure, Fe²⁺ concentration and flow velocity.

However, most of the FeCO₃ film formation studies were done by inducing film formation through the addition of Fe²⁺ ions into the test solution. These studies are not simulating the natural film forming environment in the field operations. The results based on induced film formation is not accurate because the increase of Fe²⁺ ions in the solution will accelerates the precipitation rate thus help to reduce the corrosion rate significantly which is not the case in natural film forming environment.

The following literature review attempt to give an overview of CO₂ corrosion, formation of protective FeCO₃ film in natural film forming environment and induced film forming environment and electrochemical measurement techniques used in this project.

2.1 Overview of Carbon Dioxide Corrosion

2.1.1 Mechanism of Carbon Dioxide Corrosion

Dry CO₂ gas by itself is not corrosive at the temperatures encountered within oil and gas production systems. It becomes corrosive when dissolved in an aqueous phase through which it can promote an electrochemical reaction between steel and the contacting aqueous phase. Various mechanisms have been postulated for the CO₂ corrosion process but all involve either carbonic acid (H₂CO₃) or the bicarbonate ion (2HCO₃⁻) formed on dissolution of CO₂ in water [1]. The step for the CO₂ corrosion process is presented by the reaction shown in the equations as follows:



The mechanism suggested by de Waard is:



With the steel reacting:



The overall equation is:



Besides, CO₂ corrosion also results from the practice of pumping CO₂ saturated water into wells to enhance oil recovery and reduce the viscosity of the pumped fluid. The presence of CO₂ in solution leads to the formation of a weak carbonic acid which drives CO₂ corrosion reactions [2]. The initiating process is presented by the reaction shown in equation (2.6).



The following corrosion process is controlled by three cathodic reactions and one anodic reaction. The cathodic reactions, include (2.7a) the reduction of carbonic acid into bicarbonate ions, (2.7b) the reduction of bicarbonate ions, and (2.7c) the reduction of hydrogen ions



The anodic reaction significant in CO₂ corrosion is the oxidation of iron to ferrous (Fe²⁺) ion given in equation (2.8).



These corrosion reactions promote the formation of FeCO₃ which can form along a couple of reaction paths. First, it may form when ferrous ions react directly with carbonate ions as shown in equation (2.9). However, it can also form by the two processes shown in equations (2.10a, 2.10b). When ferrous ions react with bicarbonate ions, ferrous iron bicarbonate forms which subsequently dissociates into iron carbonate along with carbon dioxide and water.



The significance of FeCO₃ formation is that it drops out of solution as a precipitate due to its limited solubility. This precipitate has the potential to form passive films on the surfaces of carbon steel which may reduce their corrosion.

2.1.2 Types of Carbon Dioxide Corrosion Damage

Typically, CO₂ corrosion damage on carbon steel could be categorized into three (3) forms which are pitting, mesa attack or flow induced localized corrosion.

1. Pitting

Pitting is defined as corrosion of a metal surface, confined to a point or small area that takes the form of cavities. Pitting can occur over the full range of operating temperatures under stagnant to moderate flow

conditions. Pitting may arise close to the dew point and can relate to condensing conditions. The susceptibility to pitting increases and time for pitting occur decrease with increasing temperature and increasing CO₂ partial pressure.

2. Mesa type attack

It is a form of localized CO₂ corrosion occurs under medium flow conditions where the formation of protective FeCO₃ film layers is unstable. Film formation begins around 60°C and thus mesa attack is much less of a concern at temperatures below this. The type of this attack most encountered in the area which is has high fluid turbulence such as welds, tubing joints, or ends/constrictions in piping.

3. Flow induced localized corrosion (FILC)

The damage is an extension of pitting and mesa attack above critical flow intensities. The localized attack propagates by local turbulence created by pits and steps at the mesa attack which act as flow disturbances. The local turbulence combined with these stresses inherent in the scale may destroy existing scales. The flow conditions may then prevent protective FeCO₃ film layers on the exposed metal to reform again.

2.1.3 Parameters Affecting Carbon Dioxide Corrosion

CO₂ corrosion is affected by several parameters including environmental, metallurgical and hydrodynamics parameters. Important parameters that affect CO₂ corrosion includes:

1. Water wetting

For CO₂ corrosion to occur there must be water present and it must wet the steel surface. The severity of CO₂ corrosion attack is proportional to the time during which the steel surface is wetted by the water phase.

2. CO₂ partial pressure

CO₂ corrosion results from the reaction of a steel surface with carbonic acid arising from the solution of CO₂ in aqueous phase. The concentration of CO₂ in the aqueous phase is directly related to the partial pressure of CO₂ in the gas in equilibrium with the aqueous phase. Thus, in CO₂ corrosion, estimates of corrosion rate are based on the partial pressure of CO₂ in the gas phase.

3. Temperature

The corrosion of carbon steel in a wet CO₂ environment can lead to formation of iron carbonate as a reaction product. At high temperatures around 80°C, the iron carbonate solubility is decreased to such extents that formation of protective FeCO₃ film layers is more likely. Under laboratory conditions, rates of uniform corrosion are consistently reduced at high temperature.

4. pH

The pH value is an important parameter in corrosion of carbon steel. The pH affects both the electrochemical reactions and the precipitation of corrosion products. Under certain production conditions the associated aqueous phase can contain salts which will buffer the pH. This tends to decrease the corrosion rate and lead to conditions under which the precipitation of protective FeCO₃ film layers is more likely.

5. H₂S content

Leaving aside the corrosion problems associated with sour systems, H₂S can have a beneficial effect on wet hydrocarbon CO₂ corrosion as sulfide scales can give protection to the underlying steel. The effect is not quantified but it does mean that facilities exposed to gas containing low levels of H₂S may often corrode at a lower rate than completely sweet systems in which the temperatures and CO₂ partial pressure are similar.

6. Carbonate film formation

Recent work on protective FeCO₃ film layers shows that the formation of these layers on the steel surface will reduce the corrosion rate. The formation and protectiveness of the film layers depends on a few parameters that are described in Section 2.2.1.

2.2 Iron Carbonate Film Formation

For many production and transportation facilities in oil and gas, the use of carbon steel is limited by CO₂ corrosion. Protective FeCO₃ film layers can form in wet CO₂ systems at all temperatures provided that the pH and the dissolved FeCO₃ concentration in the bulk are sufficiently high. The growth of FeCO₃ is a slow temperature dependent process. A high supersaturation of Fe²⁺ and CO₃²⁻ is therefore necessary in order to form a protective film layers. Once the film is formed, however, it will remain protective at much lower supersaturation [3].

As mentioned earlier, protective FeCO₃ film layers form on the steel surface if the product of Fe²⁺ and CO₃²⁻ exceeds the solubility product limit according to the following reaction:



Iron carbonate film growth depends primarily on the precipitation rate R_{FeCO_3} . As more iron carbonate precipitates the film grows in density as well as thickness. When the rate of precipitation at the steel surface equals or exceeds the rate of corrosion dense protective films form - sometimes very thin but still protective. This phenomenon has been previously quantified through the use of a non-dimensional parameter termed "scaling tendency" [4].

$$ST = \frac{R_{\text{FeCO}_3}}{CR} \quad (2.12)$$

which describes the relative rates of precipitation and corrosion expressed in the same volumetric units. For $ST \ll 1$ porous and unprotective films are likely to form, and

conversely when $ST \geq 1$ conditions become favorable for formation protective iron carbonate films. However, the use of scaling tendency is not as easy as it appears. Still needs to compute the scaling tendency at the steel surface where the films form. Furthermore, the scaling tendency changes with time as the corrosion and precipitation rate change.

In an addition, the solubility product, K_{sp} of $FeCO_3$ and supersaturation level, SS are related by the following equation:

$$SS = \frac{[Fe^{2+}][CO_3^{2-}]}{[K_{sp}]} \quad (2.13)$$

The formation of $FeCO_3$ film layers will eventually lead to the reduction of the corrosion rate. However, the exact corrosion reduction is difficult to predict in view of many factors involved such as temperature, pH, CO_2 partial pressure, Fe^{2+} concentration and flow velocity.

2.2.1 Parameters Affecting $FeCO_3$ Film Formation

As mentioned earlier, the formation of protective $FeCO_3$ film layers are affected by several parameters such as temperature, pH, CO_2 partial pressure, Fe^{2+} concentration and flow velocity. The chemistry of both formation and dissolution of corrosion products, rates of chemical reactions and transportation rates of species involved in CO_2 corrosion can be affected by the parameters described above. Some of the importance parameters in $FeCO_3$ film formation are summarized below:

1. The effect of pH

It was shown that pH has a strong influence on the conditions leading to the formation of protective $FeCO_3$ film layers. High pH results in a decreased solubility of $FeCO_3$, increased supersaturation and consequently higher precipitation rate and surface scaling tendency which resulted in faster formation of more protective $FeCO_3$ film layers that leads to the decrease in corrosion rate.

2. The effect of temperature

Prior to any FeCO_3 film layers formation the corrosion rate increases with temperature. However, at temperature of 80°C and higher, corrosion rate will start decreases as a very dense and thick protective FeCO_3 film layers formed.

3. The effect of CO_2 partial pressure

In the conditions where the formation of protective FeCO_3 film layers is favorable, increased CO_2 partial pressure will decrease corrosion rate. Given that the pH is high enough, higher CO_2 partial pressure leads to an increase in CO_3^{2-} concentration and a higher supersaturation which accelerates precipitation and FeCO_3 film layers formation.

4. The effect of Fe^{2+} concentration

The increase of Fe^{2+} concentration results in higher supersaturation, which consequently accelerates the precipitation rate and leads to higher surface scaling tendency which reduces the corrosion rate.

5. The effect of flow velocity

High flow velocity leads to increase in corrosion rate as it transports Fe^{2+} ions away from carbon steel surface, leads to a lower concentration of Fe^{2+} ions at carbon steel surface and prevents the formation of protective FeCO_3 film layers.

It is clearly mentioned that a full description of the influence of precipitation on corrosion rate is far too complicated. However, the prediction of corrosion rate is still possible under specific conditions. A further study shows that corrosion can only be reduced if the precipitation rate is of the order of the corrosion rate. In order to predict the CO_2 corrosion rate successfully, the following aspects should be clarified such as (1) protective FeCO_3 film formation, (2) the stability of these layers, (3) adherence to the steel surface of these layers and (4) repair of damaged scales. The ability of

damaged scales to self-repair has greatly influenced the reliability of protective FeCO_3 film formation [5].

2.3 Electrochemical Measurement Techniques

It is important to measure and predict CO_2 corrosion rate as it would determine the materials to be used for production and transportation facilities, in the oil and gas industry. In this project, the effect of FeCO_3 film formation on CO_2 corrosion rate will be analyzed using EIS and LPR and all the data obtained from the experiments would assist in providing a reliable prediction on the behavior of CO_2 corrosion that will lead to cost-effective and safe design of production and transportation facilities used in the oil and gas industry.

2.3.1 Electrochemical Impedance Spectroscopy (EIS)

An important advantage of EIS technique over other laboratory techniques is the possibility of using very small amplitude signals without significantly disturbing the properties being measured. In recent years, EIS technique has found widespread applications in the field of characterization of materials. It is routinely used in the characterization of coatings, batteries, fuel cells and corrosion phenomena. It has also been used extensively as a tool for investigating mechanisms in electrodeposition, electrodisolution, passivity and corrosion studies [6].

An electrochemical process may often be modeled by linear circuit elements such as resistors, capacitors, and inductors. For example, the corrosion reaction itself can often be modeled by one or more resistors. The ability to model a corrosion process in this manner gives rise to one practical attribute of the electrochemical impedance technique. Simple AC circuit theory in terms of circuit analogues can be used to model the electrochemical corrosion process. Such modeling can facilitate understanding and lead to better prediction of corrosion rates and overall corrosion behavior [7].

The fundamental approach of impedance techniques is to apply a small amplitude sinusoidal excitation signal usually a voltage between 5 to 10 mV which is applied to the working electrode over a range of frequencies, ω of 0.001 Hz to 100,000 Hz [8-9]. The current is measured. The applied voltage is divided by this measured current. Since both the voltage and current have a sinusoidal component with respect to time and are usually out-of-phase, the division results in the electrochemical impedance $Z(\omega)$, which itself has real and imaginary contributions. Often, the current is divided by the surface area and the impedance has the units of ohm-cm². The electrochemical impedance $Z(\omega)$, is the frequency dependent proportionality factor that act as a transfer function by establishing a relationship between the excitation voltage signal and the current response of the system shown in equation (2.14).

$$Z(\omega) = E(\omega)/I(\omega) \tag{2.14}$$

The magnitude of the resistance or opposition to the current created by capacitors and inductors is dependent on the frequency while the magnitude of the opposition created by the resistor is independent of frequency.

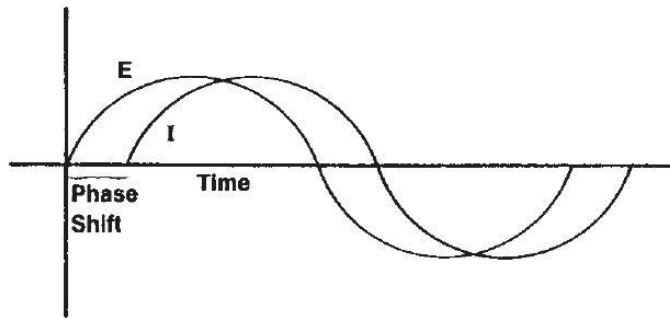


Figure 2.1: Sinusoidal AC voltage and current signals

The technique can be described in terms of a response to a frequency dependent input signal. When a voltage sine or cosine wave is applied across a circuit composed of a resistor only, the resultant current is also a sine or cosine wave of the same frequency with no phase angle shift but with an amplitude which differs by an amount determined by the proportionality factor. In contrast, if the circuit consists of capacitors and inductors, the resulting current not only differs in

amplitude but is also shifted in time. It has a phase angle shift. This phenomenon is shown in Figure 2.1.

Vector analysis can be used to describe the equivalent circuit in mathematical terms. The relationship between such vector analysis and imaginary or complex numbers provides the basis for electrochemical impedance analysis. A sinusoidal current or voltage can be viewed as a rotating vector as shown in Figure 2.2. It shows that the current vector rotates at a constant angular frequency f (hertz) or ω (radians/s = $2\pi f$). The x component defines the in-phase current. Therefore, it becomes the “real” component of the rotating vector. The y component is shifted out-of-phase by 90° . By convention, it is termed the “imaginary” component of the rotating vector.

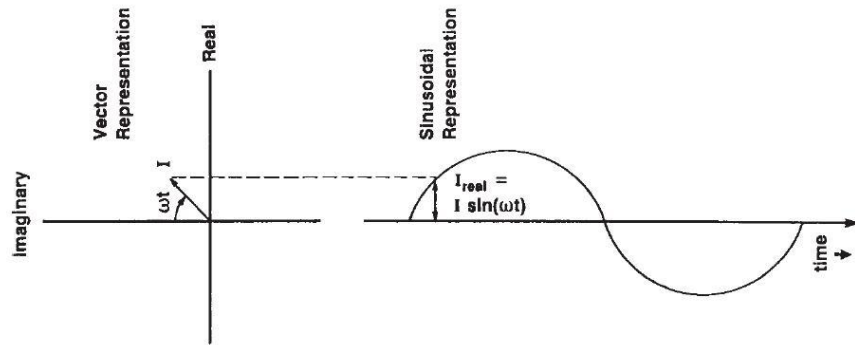


Figure 2.2: Relationship between sinusoidal AC current and rotating vector representation

The mathematical description of the two components is described in below equation:

$$\text{Real Current} = I_x = |I| \cos(\omega t) \quad (2.15)$$

$$\text{Imaginary Current} = I_y = |I| \sin(\omega t) \quad (2.16)$$

$$|I|^2 = |I_x|^2 + |I_y|^2 \quad (2.17)$$

The voltage can be pictured as a similar rotating vector with its own amplitude, E and the same rotation speed, ω .

As shown in Figure 2.3, when the current is in phase with the applied voltage, the two vectors are coincident and rotate together. This response is characteristic of a circuit containing only a resistor. When the current and voltage are out-of-phase, the two vectors rotate at the same frequency, but they are offset by an angle called the phase angle, θ . This response is characteristic of a circuit which contains capacitors and inductors in addition to resistors.

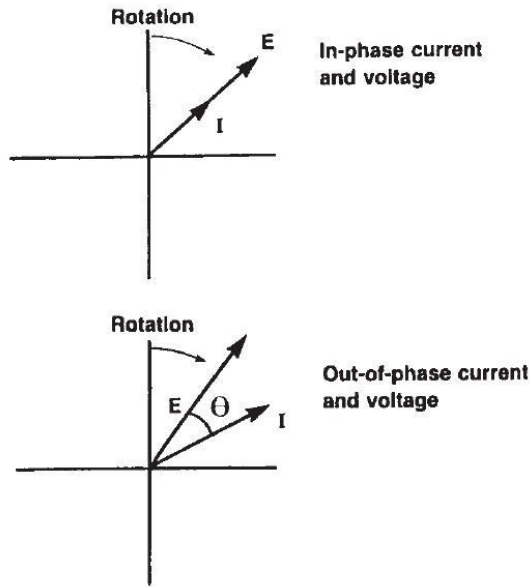


Figure 2.3: In-phase and out-of-phase rotation of current and voltage vectors

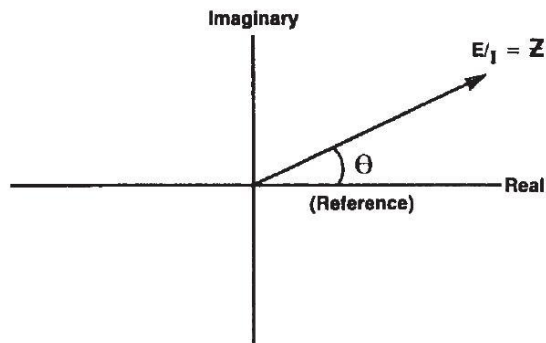


Figure 2.4: Impedance vector

In electrochemical impedance analysis, both the current and voltage vectors are referred to the same reference frame. The voltage vector is “divided” by the current

vector to yield the final result in terms of the impedance as shown in Figure 2.4. The impedance is the proportionality factor between the voltage and the current.

The mathematical convention for separating the real (x) and imaginary (y) components is to multiply the magnitude of the imaginary contribution by j and report the real and imaginary values as a complex number. The equations for electrochemical impedance become:

$$E = E_{real} + E_{imaginary} = E' + jE'' \quad (2.18)$$

$$I = I_{real} + I_{imaginary} = I' + jI'' \quad (2.19)$$

$$Z = Z' + jZ'' = (E' + jE'') / (I' + jI'') \quad (2.20)$$

$$\tan \theta = Z''/Z' \quad (2.21)$$

$$|Z|^2 = (Z')^2 + (Z'')^2 \quad (2.22)$$

The goal of the electrochemical impedance technique is to measure the impedance Z as a function of frequency and to derive corrosion rate or mechanism information from the values. Use of simple circuit analogues to model the response is one methodology to achieve this goal. The amplitude of the excitation signal must be small enough so that the response is linearly related to the input, that is, the response is independent of the magnitude of the excitation.

Table 2.1: Circuit elements

Element	Equation
Resistor	$Z = R$
Capacitor	$Z = 1/(j\omega C)$
Inductor	$Z = j\omega L$

The three basic circuit elements can be written as shown in Table 2.1. It shows that a resistor has a real contribution only. That is, the response of a resistor would be a point on the real axis, independent of frequency. Both the capacitor and inductor have purely imaginary contributions. These would appear on the imaginary axis only. One method of electrochemical impedance analysis is to model the corrosion

process in terms of circuit elements such as those shown in Table 2.1 and from that model to make conclusions about the physics of corrosion.

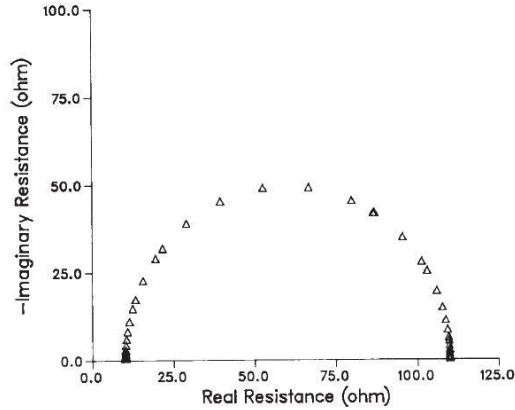


Figure 2.5: Nyquist plot

The plot of the real part of impedance against the imaginary part gives a Nyquist plot as shown in Figure 2.5. The advantage of Nyquist representation is that it gives a quick overview of the data and one can make some qualitative interpretations. While plotting data in the Nyquist format, the real axis must be equal to the imaginary axis so as not to distort the shape of the curve which is important in making qualitative interpretations of the data.

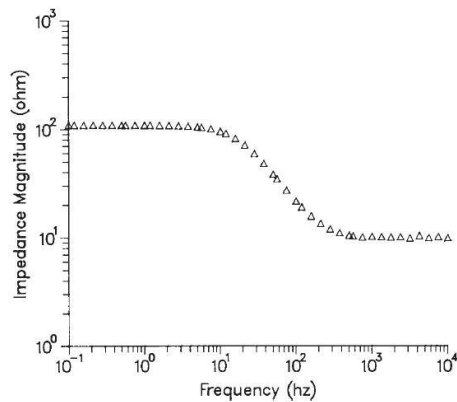


Figure 2.6: Impedance vs. frequency

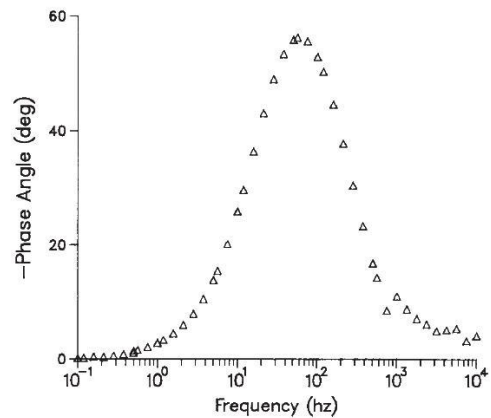


Figure 2.7: Phase angle vs. frequency

The disadvantage of the Nyquist presentation is that one loses the frequency dimension of the data. One way of overcoming this problem is by labeling the frequencies on the curve. The absolute value of impedance and the phase shifts are plotted as a function of frequency in two different plots giving a Bode plot, as shown in Figure 2.6 and Figure 2.7.

2.3.2 Simple Corrosion Process

The simplest type of corrosion process would be a combination of a corrosion reaction consisting of two simple electrochemical reactions and a double layer. Corrosion would proceed uniformly on the surface. For example, the corrosion of carbon steel in 1 M sulfuric acid can be considered to fall into this category shown in equation (2.23):



This reaction may be represented by a simple resistor. The double layer is created by the voltage change across the interface. On the metal side of the interface, there may be an excess (or deficiency) of electrons. This excess (or deficiency) is balanced on the solution side by oppositely charged ions. Some are specifically adsorbed at the surface (inner layer). Others are nonspecifically adsorbed and are hydrated. They extend out into the solution in the diffuse layer. The response of this interfacial structure to varying voltage (for example sinusoidal excitation) can be modeled by a capacitor, the double layer capacitance.

For this simple process, the model circuit shown in Figure 2.8. The circuit consists of a resistor R_p in parallel with a capacitor C . The entire parallel circuit is in series with another resistor R_s . The utility of this model for the frequency response lies in the fact that R_s equals the solution resistance not compensated by the potentiostat and R_p equals the polarization resistance as long as the measurement is made at the corrosion potential. By combining R_p with the Tafel slopes for the half-cell reactions by an equation such as the Stern-Geary equation, the corrosion rate can be estimated. Thus, analysis of electrochemical impedance enables the corrosion rate

to be estimated rapidly in the absence of uncompensated solution resistance when the measurement is made at the corrosion potential.

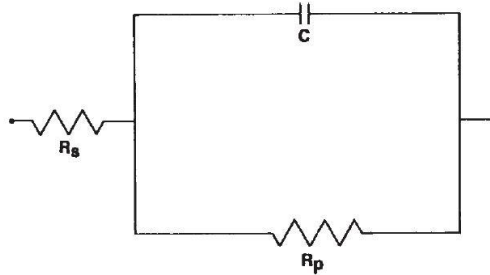


Figure 2.8: Circuit that models simple impedance response

2.3.3 Diffusion Control

Sometimes the rate of a chemical reaction can be influenced by the diffusion of one or more reactants or products to or from the surface. This situation can arise when diffusion through a surface film or hydrodynamic boundary layer becomes the dominating process. Examples are the surface being covered with reaction products of limited solubility. An example of this type of corrosion process that has extreme practical importance is the corrosion of carbon steel in concentrated sulfuric acid in which the product FeSO_4 has limited solubility. Such corrosion has been shown to be controlled by the diffusion of FeSO_4 from a saturated film at the surface to the bulk fluid. Very often, electrochemical impedance data for such systems has a unique characteristic known as the Warburg impedance. In the low frequency limit, the current is a constant 45° out-of-phase with the potential excitation. The impedance response should ultimately deviate from this relationship. It will return to the real axis at very low frequencies that may be impossible to measure. The equivalent circuit is shown in Figure 2.9.

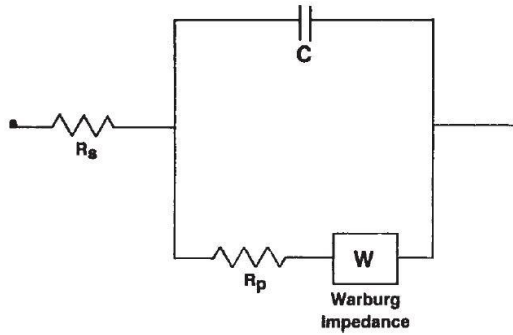


Figure 2.9: Circuit that models impedance in the presence of diffusion

The term W is the Warburg impedance. By appropriate manipulation of the data, the values of the circuit elements can be evaluated. These circuit elements can be used to obtain a value for a resistance (charge transfer resistance) that can sometimes be related to a corrosion rate.

2.3.2 Linear Polarization Resistance (LPR)

The electrochemical technique, commonly referred to as Linear Polarization Resistance, is the only corrosion monitoring method that allows corrosion rates to be measured directly, in real time. The polarizing voltage of 10 mV has been chosen as being well within the limits for which the linear relationship between I_{CORR} and $\Delta E/\Delta I$ holds. Additionally, the value is sufficiently small as to cause no significant or permanent disruption of the corrosion process, so that subsequent measurements remain valid.

Anodic and cathodic sites continually shift position, and they exist within a continuously conductive surface, making direct measurement of i_{CORR} impossible. Small, externally-imposed, potential shifts (ΔE) will produce measurable current flow (ΔI) at the corroding electrode. The behavior of the externally imposed current is governed, as is that of i_{CORR} , by the degree of difficulty with which the anodic and cathodic corrosion processes take place.

Therefore the greater difficulty will give smaller value of i_{corr} and ΔI for a given potential shift. In fact, at small values of ΔE , ΔI is directly proportional to i_{corr} , and hence to the corrosion rate. This relationship is embodied in the theoretically derived Stern-Geary equation:

$$\frac{\Delta E}{\Delta I} = \frac{\beta_a \beta_c}{2.3(i_{\text{corr}})(\beta_a + \beta_c)}$$

where β_a and β_c are the Tafel slopes of the anodic and cathodic reactions respectively.

CHAPTER 3 METHODOLOGY

3.1 Research Methodology

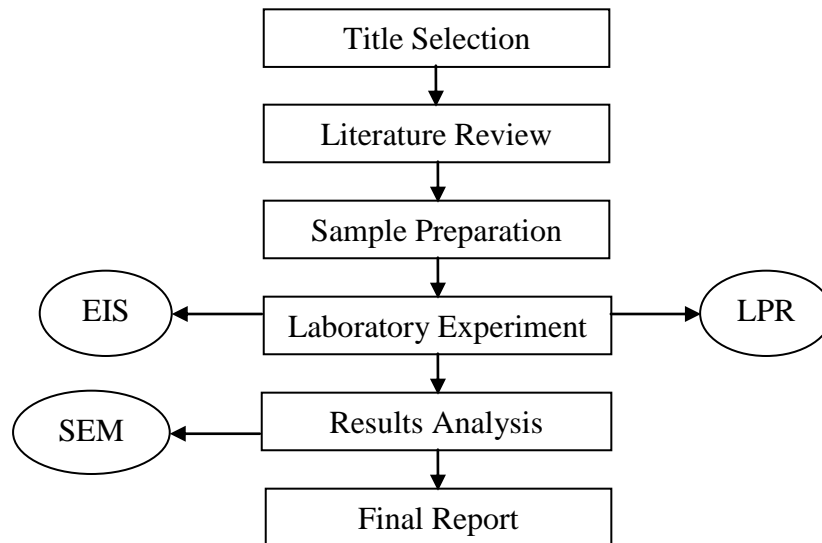


Figure 3.1: Project flow chart

From Figure 3.1, it shows the project flow chart where research were done on some resources such as books, journals and technical papers specifically on CO₂ corrosion of carbon steel, protective FeCO₃ film formation and EIS technique. Besides, consultation sessions with the supervisor and related personnel were also held in order to get a better understanding on the EIS technique. The laboratory experiments were conducted on BS 970 steel in stagnant condition using 3 wt% NaCl over a series of parameters which includes temperature, partial pressure of CO₂, Fe²⁺ concentration and flow velocity. EIS and LPR techniques were employed to study and analyze CO₂ corrosion rate and formation of protective FeCO₃ film layers. Once the results were obtained, analysis was done using SEM technique. Lastly, final report was written to complete this project.

3.2 Electrochemical Measurement Techniques

3.3.1 Electrochemical Impedance Spectroscopy (EIS)

The fundamental approach of EIS technique is to apply a small amplitude sinusoidal excitation signal usually a voltage between 5 to 10 mV which is applied to the working electrode over a range of frequencies, ω of 0.001 Hz to 100,000 Hz. The usual result is a Nyquist plot of half a semi-circle, the high frequency part giving the solution resistance and the width of the semi-circle giving the corrosion rate in the same manner as LPR. The analysis of this data is performed by circle fitting in the analysis software. One useful benefit of EIS technique is the ability to measure the solution resistance at high frequency.

3.3.2 Linear Polarisation Resistance (LPR)

This technique is based on the linear approximation of the polarization behavior at potentials near the corrosion potential. R_p is given by Stern and Geary equation:

$$R_p = \frac{\Delta E}{\Delta I} = \frac{\beta_A \beta_C}{(\beta_A + \beta_C) i_{corr}}$$

$$i_{corr} = \frac{B}{R_p}, \text{ Where } B = \frac{\beta_A \beta_C}{(\beta_A + \beta_C)}$$

$$ba = 2.3\beta_A \text{ and } bc = 2.3\beta_C; B = abc / 2.3(ba + bc)$$

The corrosion current can be related directly to the corrosion rate from Faraday's law:

$$CR(mm/year) = \frac{315 \times Z \times i_{corr}}{\rho \times n \times F}$$

Where,

CR = Corrosion Rate (mm/year)

i_{corr} = Corrosion current density, $\frac{\mu A}{cm^2}$

ρ = Density of iron, 7.8 g/cm³

F = Faraday's constant, 96,500 C/mole

Linear polarization resistance measurements were performed by firstly measuring the corrosion potential of the exposed sample and subsequently sweeping from -10 mV to + 10 mV with the sweep rate 10 mV/min.

3.3 Materials

The working electrode was made from BS 970 low carbon steel. The detailed chemical composition of the carbon steel is given in Table 3.3.

Table 3.1: Chemical composition of BS 970

Steel	C (%)	Si (%)	Mn (%)	P (%)	S (%)	Cr (%)	Mo (%)	Ni (%)	Fe (%)
BS 970	0.148	0.175	0.799	0.010	0.032	0.069	0.014	0.065	Balance

3.4 Sample Preparation

The working electrode as shown in Figure 3.2 was machined from the parent material into the cylindrical shape and had a diameter of 1.2 cm and thickness of 0.5 cm with the exposed area of 1.131 cm², Figure 3.3. The steps of fabricating the test specimens involved a few steps. Firstly, the test specimens were spot welded with copper wire with certain length usually around 30 cm. Then, the test specimens were mounted with epoxy by cold mounting as shown in and grinded with wet silicon carbide (SiC) paper with a final wet grind using 600 grit SiC paper, Figure 3.4 and Figure 3.5. Finally, the

test specimens were rinsed with deionizer water and degreased with acetone prior to immersion.



Figure 3.2: The working electrode



Figure 3.3: The exposed area



Figure 3.4: Sample cold mounting

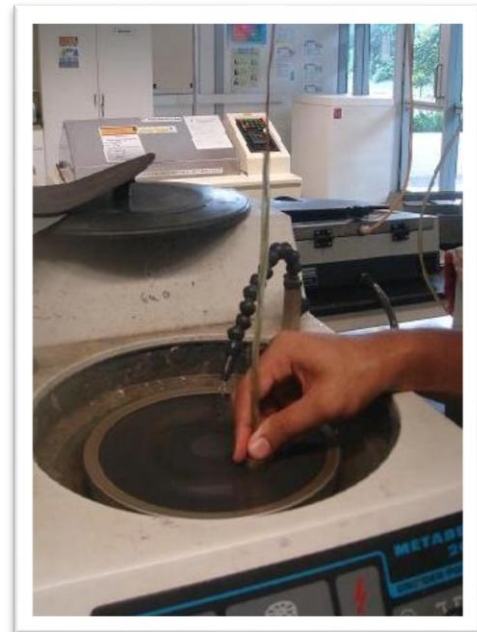


Figure 3.5: Metallurgical grinder

3.5 Test Environment

For natural film forming environment, all experiments were carried out in CO_2 saturated 3% NaCl solution by purging CO_2 for at least one hour prior to each experiment to remove the dissolved oxygen from the test solution. At these conditions

the saturation pH was 3.80. The pH solution could be adjusted by adding an amount of 1M NaHCO₃. For induced film forming environment, 50 ppm concentration of ions Fe²⁺ was added to the test solution. The pH value is checked by microcomputer pH-meter METTLER-TOLEDO Model 320, which had been calibrated using standard buffer solutions.

3.6 Experimental Setup

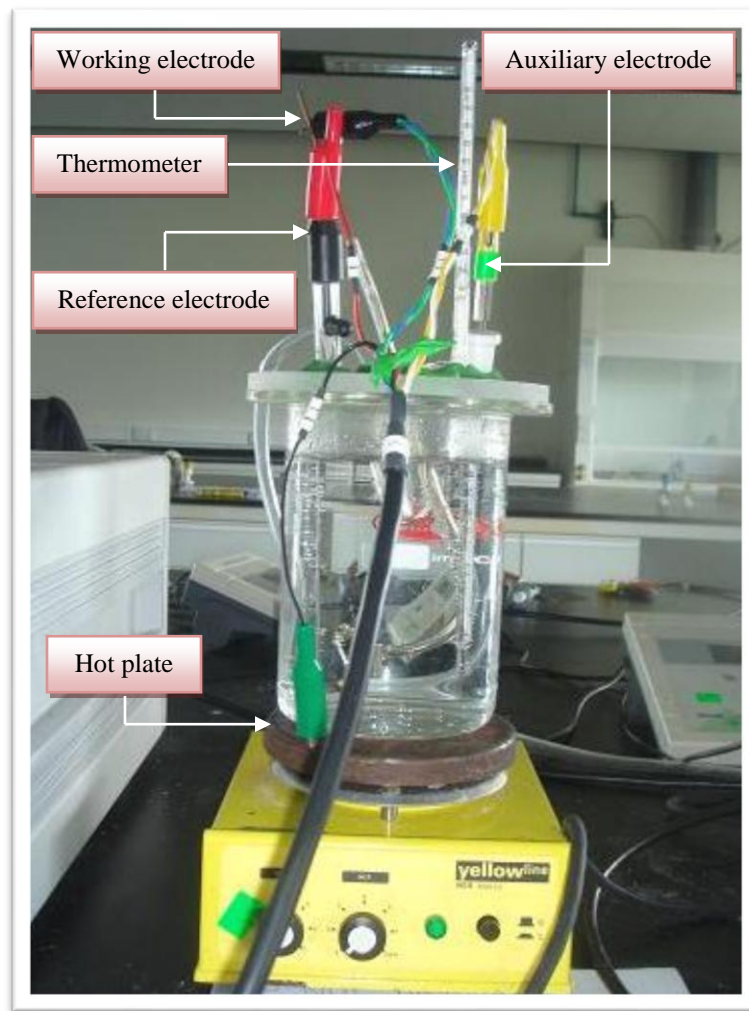


Figure 3.6: Experimental setup

The experimental setup is shown in Figure 3.2. The test assembly consists of one-liter glass cell bubbles with CO₂. The required test temperature is set through a hot plate.

The electrochemical measurements are based on a three-electrode system, using a commercially available potentiostat with a computer control system. The reference electrode used is a saturated calomel electrode (SCE) and the auxiliary electrode is a platinum electrode. The test matrix of the experiment is as shown in Table 3.2.

Table 3.2: Test matrix for the research

Parameter	Value
Steel Type	BS 970
Solution	3 % NaCl
De-oxygenation gas	CO ₂
pH	6.0
Temperature (°C)	25, 40, 60, 80
Fe ²⁺ (ppm)	0, 50
Rotational velocity (rpm)	0 / stagnant
Sand paper grit used	120, 180, 240, 400, 600
Measurement techniques	EIS, LPR, SEM

In this project, the effect of temperature (t) = 25°C, 40°C, 60°C and 80°C and Fe²⁺ concentration ($c_{Fe^{2+}}$) = 0 and 50 ppm will be specifically studied to observe how these two parameters affect the CO₂ corrosion rate and formation of protective FeCO₃ film. The other parameters such as pH, partial pressure of CO₂ and flow velocity will be set at 6.0, 1 bar and 0 rpm / stagnant, respectively. This test matrix was chosen to reflect the conditions in the field. The experiments were conducted for duration up to 24 hours in order to observe the effect of FeCO₃ film formation on CO₂ corrosion rate.

3.7 Experimental Procedure

The experimental procedure for EIS and LPR was conducted after sufficient CO₂ gas bubbling, adjusting the solution to the required pH and attaining the set temperature. The bubbling is reduced and maintained throughout the experiment.

1. Bubble CO₂ through one-litre 3% NaCl for one hour before inserting the sample.

2. Adjust pH of the solution to the required values by adding solution of 1M NaHCO₃.
pH is measured at room temperature by pH meter.
3. Set the temperature and maintain with an accuracy of $\pm 1^{\circ}\text{C}$.
4. Insert the mounted and polished sample into glass cell and run the experiment
5. For EIS, take readings at the beginning and at the end of the experiment.
6. For LPR, take readings every one hour for 24 hours.
7. Repeat the procedures for all temperatures and test environments.

CHAPTER 4

RESULTS AND DISCUSSION

The results of natural and induced film formation in CO₂ corrosion environment are presented in Section 4.1 and Section 4.2, respectively.

4.1 Natural Film Forming Environment

For natural film forming environment, all experiments were carried out in CO₂ saturated 3% NaCl solution at pH 6 using EIS, LPR and SEM techniques.

4.1.1 Electrochemical Impedance Spectroscopy (EIS)

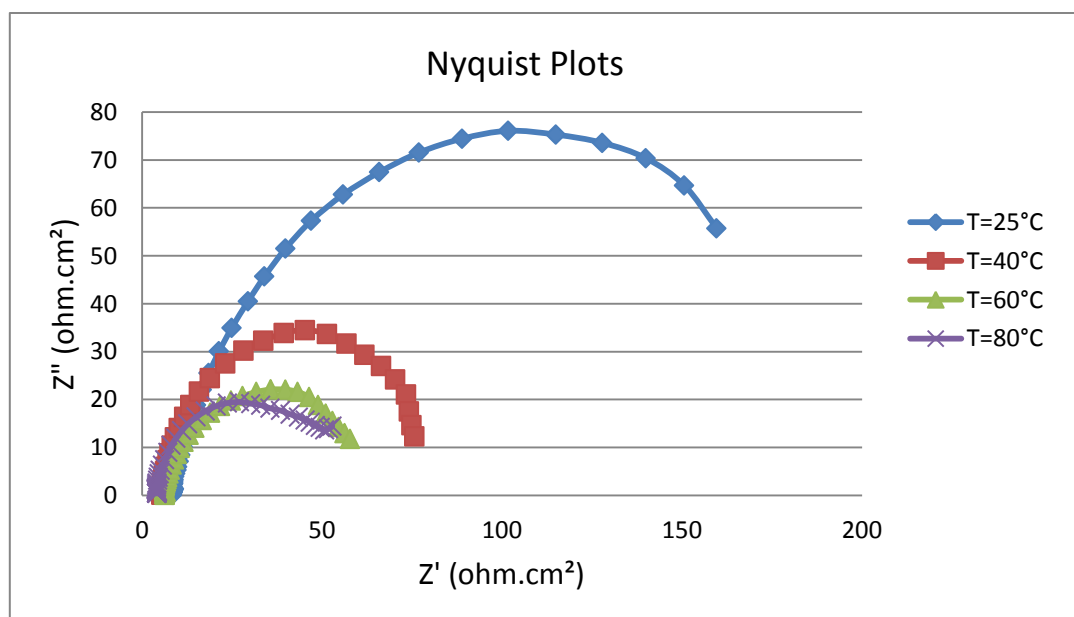


Figure 4.1: Impedance spectra, presented as a Nyquist plot, recorded for 24 hours immersion of a carbon steel specimen in CO₂ saturated 3% NaCl solution at various temperatures

A selection of typical impedance spectra, presented as Nyquist plots at various temperatures of 25°C, 40°C, 60°C and 80°C are presented in Figure 4.1. The Nyquist plots are approximately semicircular, and as the temperature increases, the semicircular diameter decreases which shows the increases in the corrosion rate. This is true for all impedance spectra of 25°C, 40°C, and 60°C but for impedance spectra at 80°C, it shows some changes of shape as shown in Figure 4.2 which describe the involvement of kinetics and diffusion processes that can relate to the formation of FeCO₃ film layers. The corrosion rate at 80°C is expected to decrease since FeCO₃ film layers are expected to start forming on the steel surface.

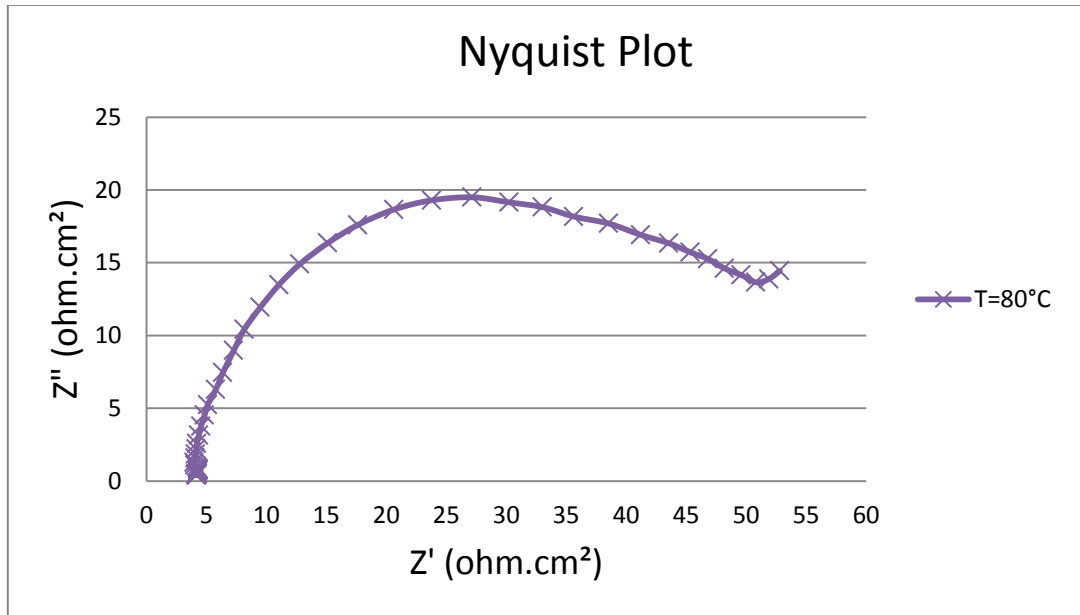


Figure 4.2: Impedance spectra, presented as a Nyquist plot, recorded for 24 hours immersion of a carbon steel specimen in CO₂ saturated 3% NaCl solution at temperature of 80°C

From Figure 4.1, the values of polarization resistance, R_p are calculated from the semicircular diameter of the Nyquist plots. These values of R_p are then used to calculate the average corrosion rate at pH 6 of a carbon steel specimen in CO₂ saturated 3% NaCl solution for all temperatures and were shown in Figure 4.3.

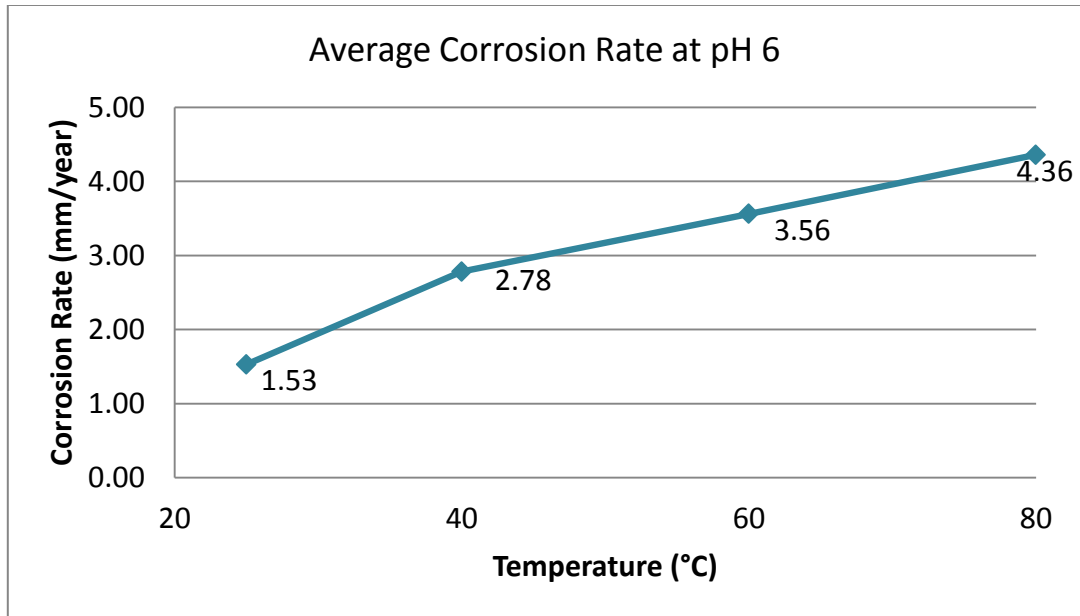


Figure 4.3: Average corrosion rate at pH 6 of a carbon steel specimen in CO₂ saturated 3% NaCl solution at various temperatures

From the results, it shows that the average corrosion rate at temperature of 25°C is the lowest with 1.53 mm/year which is then increases to 2.78 mm/year at temperature of 40°C followed by the corrosion rate at temperature of 60°C and 80°C with 3.56 mm/year and 4.36 mm/year respectively.

The corresponding Bode plots of phase angle, θ , in Figure 4.4 shows that all plots have two similar peaks at different frequencies. The peak at lower frequencies decreased with the increase of the temperature, which indicated that the interfacial structure between the electrode and the corrosive solution changed gradually with the development of the surface film. The phase angle peaks at higher frequency were mainly induced by the formation of the FeCO₃ film layers on the surface of the electrode, and the phase angle peaks at the lower frequencies might be resulted from the electrochemical process at the interfaces between metal electrode and solution [10].

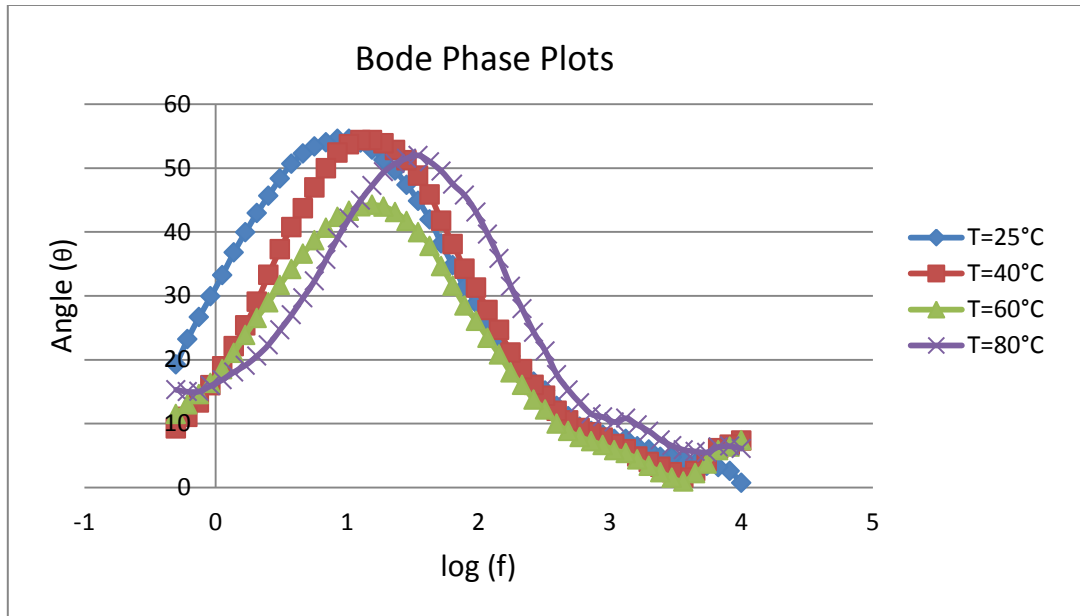


Figure 4.4: Impedance spectra, presented as a Bode plot of phase angle against frequency, recorded for 24 hours immersion of a carbon steel specimen in CO_2 saturated 3% NaCl solution at various temperatures

Figure 4.5 shows the proposed electrical equivalent circuits employed to analyze the impedance plots of (a) temperature of 25°C , 40°C , and 60°C and (b) temperature of 80°C . The parameters of interest are electrolyte resistance (R_s), double layer capacitance (C_{dl}), electrochemical charge transfer resistance (R_{ct}), and Warburg impedance (Z_w).

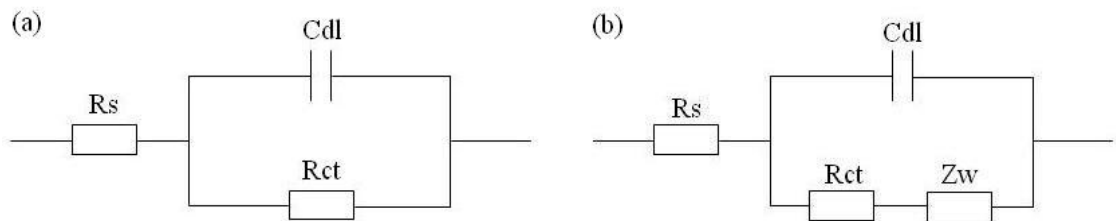


Figure 4.5: Equivalent circuits used to represent the impedance results at (a) temperature of 25°C , 40°C , and 60°C ; (b) temperature of 80°C

4.1.2 Linear Polarisation Resistance (LPR)

Figure 4.6 shows the effect of temperatures to the corrosion rate at pH 6 for 24 hours immersion of a carbon steel specimen in CO₂ saturated 3% NaCl solution at various temperatures of 25°C, 40°C, 60°C and 80°C. It shows that, after corrosion occurs for several hours, the corrosion rate started to decrease smoothly at eight (8) hours of experiment for all the temperatures. Besides, it also shows that at low temperatures (25°C, 40°C and 60°C), the corrosion rate increases as the temperature increases because of high solubility of the FeCO₃ film layers. However, as temperature increases (around 60-80°C), the FeCO₃ film layers become more adherent to the steel surface and more protective in nature resulting in a decrease of the corrosion rate. This is due to the fact that, higher temperature increases kinetic of corrosion reaction, makes the solution saturated faster. As such, corrosion rate decreases significantly at temperature of 80°C.

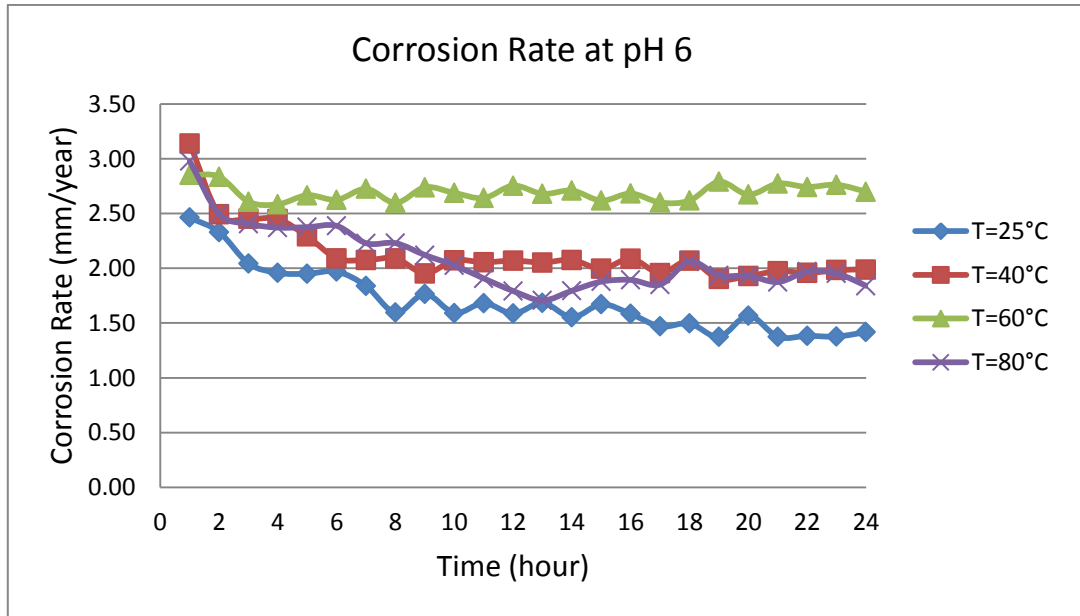


Figure 4.6: Corrosion rate at pH 6, recorded for 24 hours immersion of a carbon steel specimen in CO₂ saturated 3% NaCl solution at various temperatures

The average corrosion rate at pH 6 of a carbon steel specimen in CO₂ saturated 3% NaCl solution for all temperatures is then plotted together as shown in Figure 4.7

by taking the average value of the corrosion rate from eight (8) hours up to 24 hours of experiment for each experiment. This is done to observe the effect of temperature to the corrosion rate as it is known that increased temperature aids the formation of FeCO_3 film layers by accelerating the kinetics of precipitation. From the results, it shows that the average corrosion rate at temperature of 25°C is the lowest with 1.54 mm/year which is then increases to 2.01 mm/year at temperature of 40°C . The highest corrosion rate is 2.69 mm/year at temperature of 60°C while at temperature of 80°C , the average corrosion rate decreases back to 1.93 mm/year where FeCO_3 film layers might have been formed at the steel surface.

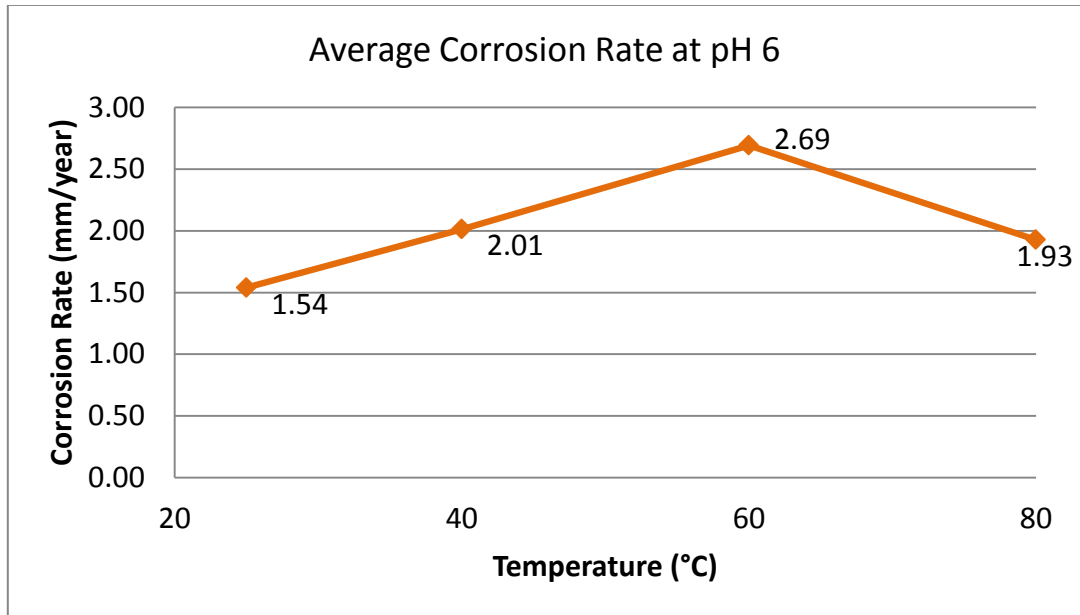
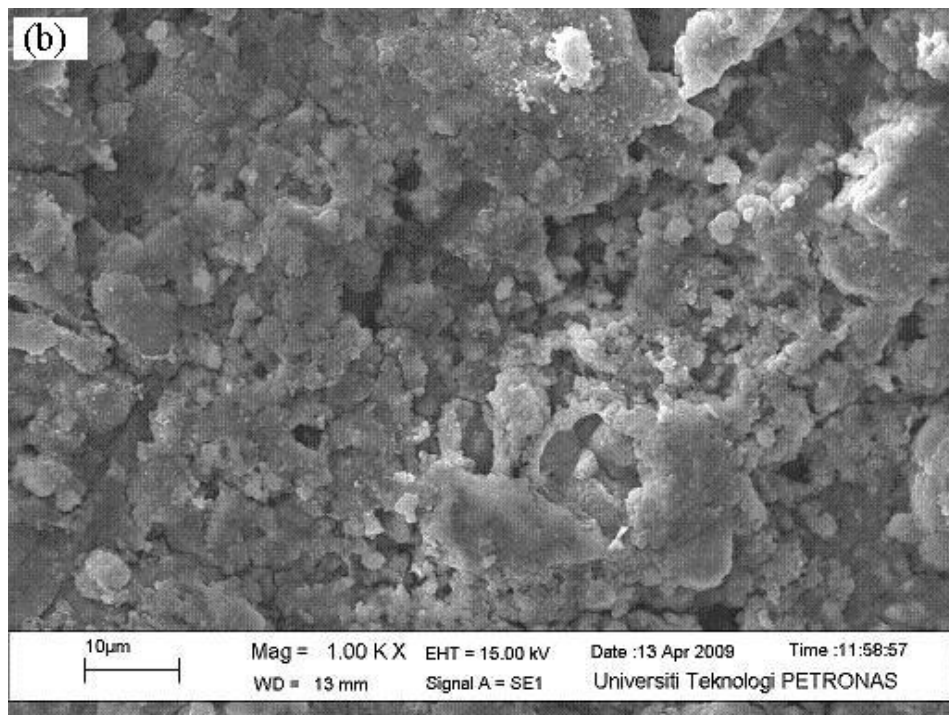
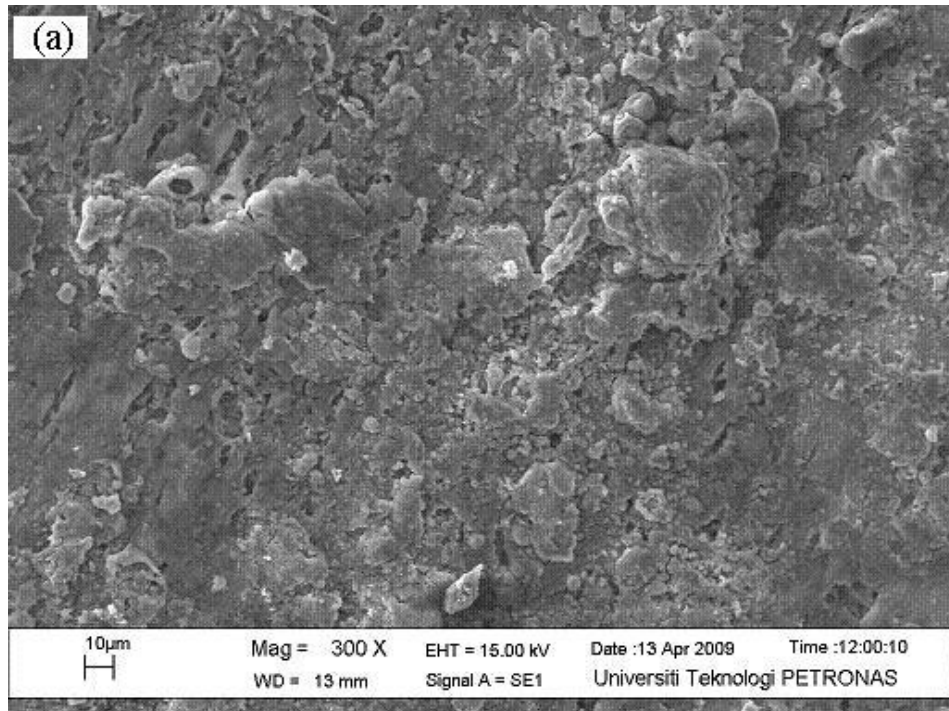


Figure 4.7: Average corrosion rate at pH 6 of a carbon steel specimen in CO_2 saturated 3% NaCl solution at various temperatures

4.1.3 Scanning Electron Microscopy (SEM)

Figure 4.8 shows the SEM images of a carbon steel specimen immersed for 24 hours in CO_2 saturated 3% NaCl solution at temperature of 80°C in different magnification of (a) 300x, (b) 1000x and (c) 3000x. It can be seen from the SEM images that the FeCO_3 film layers formed are dense but still porous due to the fact that the experiments are only being done up to 24 hours. In order to form a very

dense and protective FeCO_3 film layers, longer time of experiment is needed e.g. 48 – 96 hours.



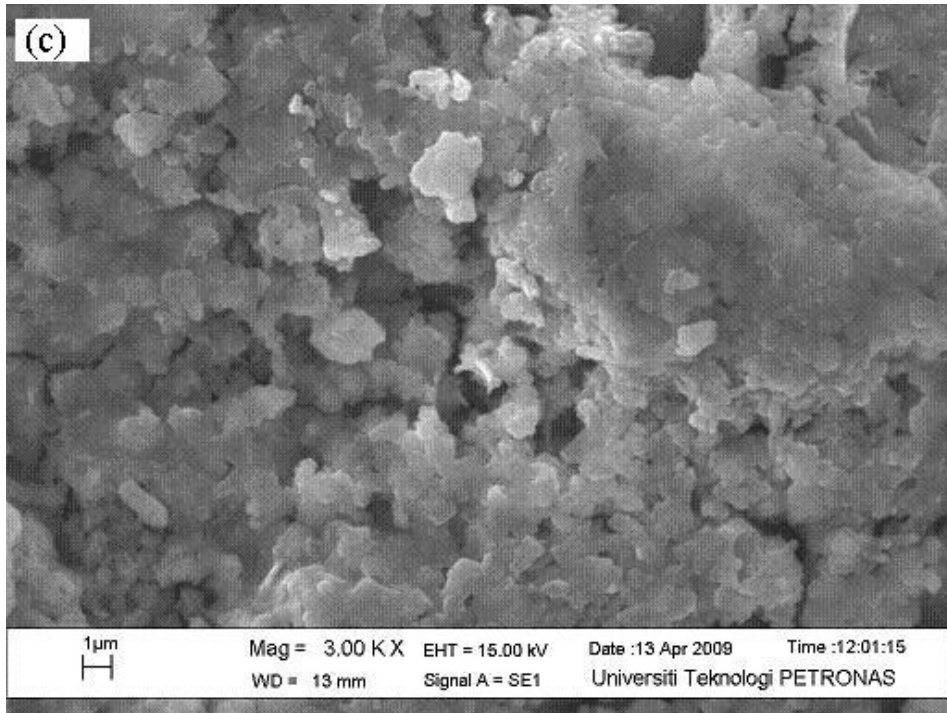


Figure 4.8: SEM images, for 24 hours immersion of a carbon steel specimen in CO₂ saturated 3% NaCl solution at temperature of 80°C (a) 300x (b) 1000x (c) 3000x

4.2 Induced Film Forming Environment

For induced film forming environment, all experiments were carried out in CO₂ saturated 3% NaCl solution at pH 6 with an addition of 50 ppm concentration of ions Fe²⁺ to the test solution using EIS, LPR and SEM techniques.

4.2.1 Electrochemical Impedance Spectroscopy (EIS)

Impedance spectra at temperatures of 25°C, 40°C, 60°C and 80°C are presented in Figure 4.9. As shown in Figure 4.9, the semicircular diameters increased significantly as compared with the semicircular diameters in Figure 4.1 which reflect to the decreases in the corrosion rate, indicating the possibility of continuous growth of FeCO₃ film layers. The Nyquist plots are approximately semicircular, and as the temperature increases, the semicircular diameter decreases which shows

the increases in the corrosion rate. This is true for all impedance spectra of 25°C, 40°C, and 60°C but for impedance spectra at 80°C, it shows some changes of shape as shown in Figure 4.10 which describe the involvement of kinetics and diffusion processes that can relate to the formation of FeCO₃ film layers. The corrosion rate at 80°C is expected to decrease since FeCO₃ film layers are expected to start forming on the steel surface.

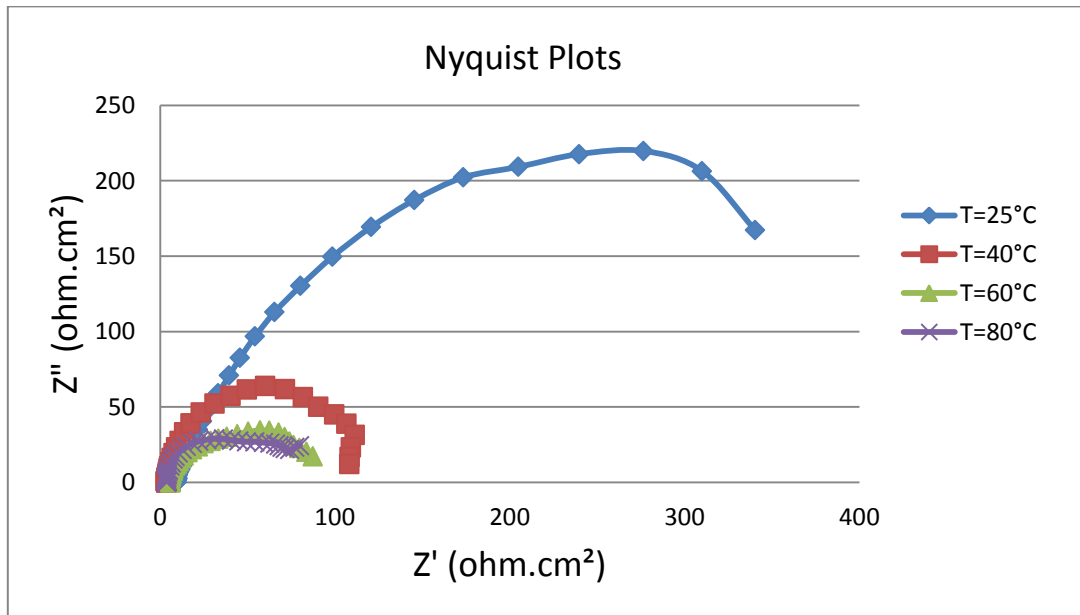


Figure 4.9: Impedance spectra, presented as a Nyquist plot, recorded for 24 hours immersion of a carbon steel specimen in CO₂ saturated 3% NaCl solution with an addition of 50 ppm concentration of ions Fe²⁺ at various temperatures

From Figure 4.9, the values of polarization resistance, R_p are calculated from the semicircular diameter of the Nyquist plots. These values of R_p are then used to calculate the average corrosion rate at pH 6 of a carbon steel specimen in CO₂ saturated 3% NaCl solution with an addition of 50 ppm concentration of ions Fe²⁺ at various temperatures and were shown in Figure 4.11.

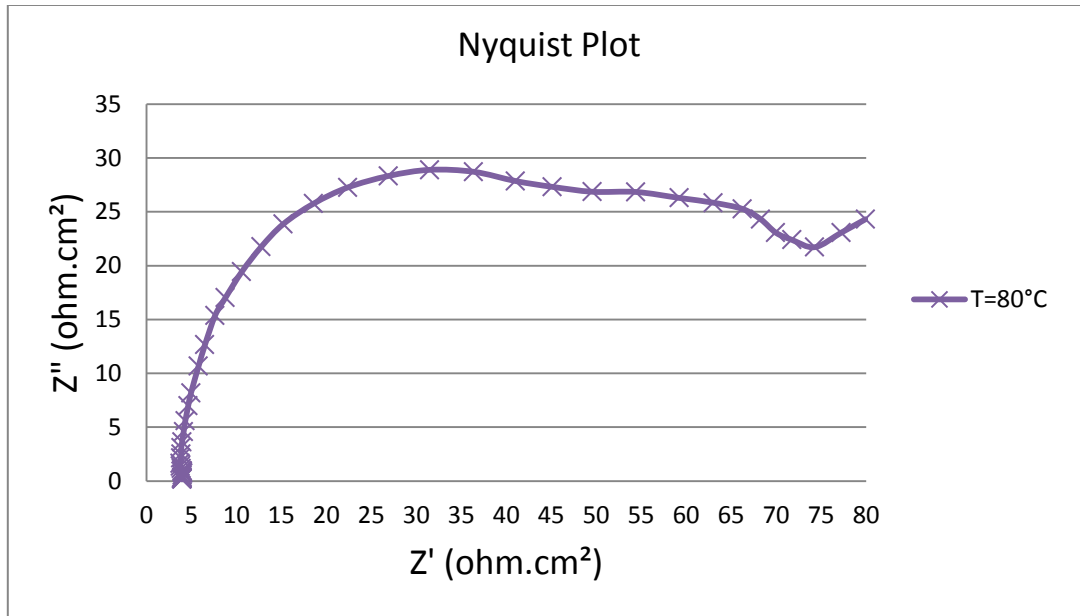


Figure 4.10: Impedance spectra, presented as a Nyquist plot, recorded for 24 hours immersion of a carbon steel specimen in CO_2 saturated 3% NaCl solution with an addition of 50 ppm concentration of ions Fe^{2+} at temperature of 80°C

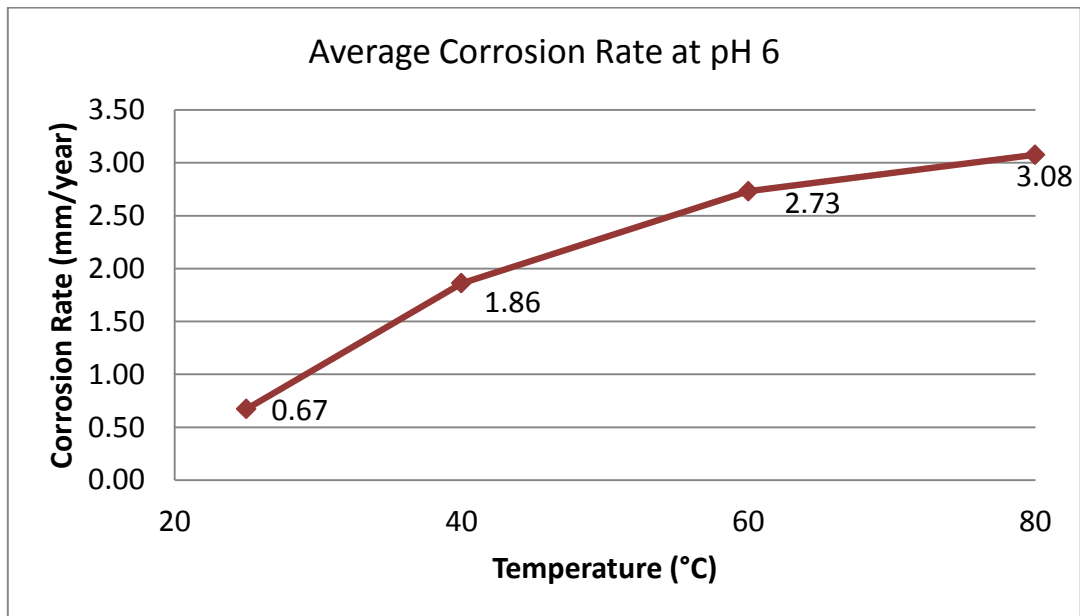


Figure 4.11: Average corrosion rate at pH 6 of a carbon steel specimen in CO_2 saturated 3% NaCl solution with an addition of 50 ppm concentration of ions Fe^{2+} at various temperatures

From the results, it shows that the average corrosion rate at temperature of 25°C is the lowest with 0.67 mm/year which is then increases to 1.86 mm/year at temperature of 40°C followed by the corrosion rate at temperature of 60°C and 80°C with 2.73 mm/year and 3.08 mm/year respectively.

The corresponding Bode plots of phase angle, θ , in Figure 4.12 shows that all plots have two similar peaks at different frequencies. The peak at lower frequencies decreased with the increase of the temperature, which indicated that the interfacial structure between the electrode and the corrosive solution changed gradually with the development of the surface film. The phase angle peaks at higher frequency were mainly induced by the formation of the FeCO_3 film layers on the surface of the electrode, and the phase angle peaks at the lower frequencies might be resulted from the electrochemical process at the interfaces between metal electrode and solution [10].

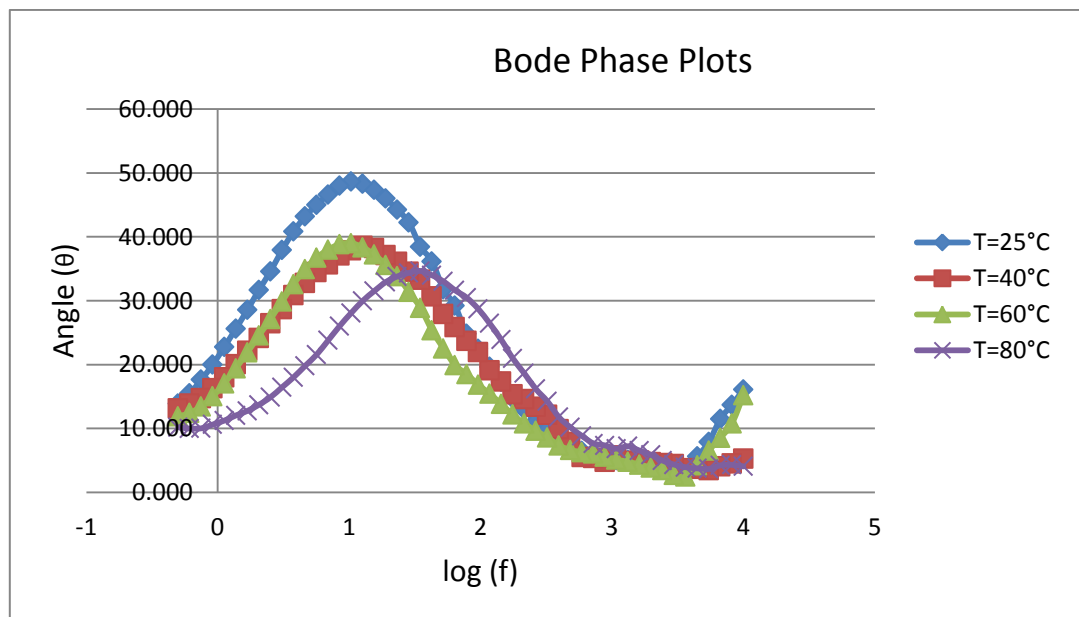


Figure 4.12: Impedance spectra, presented as a Bode plot of phase angle against frequency, recorded for 24 hours immersion of a carbon steel specimen in CO_2 saturated 3% NaCl solution with an addition of 50 ppm concentration of ions Fe^{2+} at various temperatures

Figure 4.5 shows the proposed electrical equivalent circuits employed to analyze the impedance plots of (a) temperature of 25°C, 40°C, and 60°C and (b) temperature of 80°C. The parameters of interest are electrolyte resistance (R_s), double layer capacitance (C_{dl}), electrochemical charge transfer resistance (R_{ct}), and Warburg impedance (Z_w).

4.2.2 Linear Polarisation Resistance (LPR)

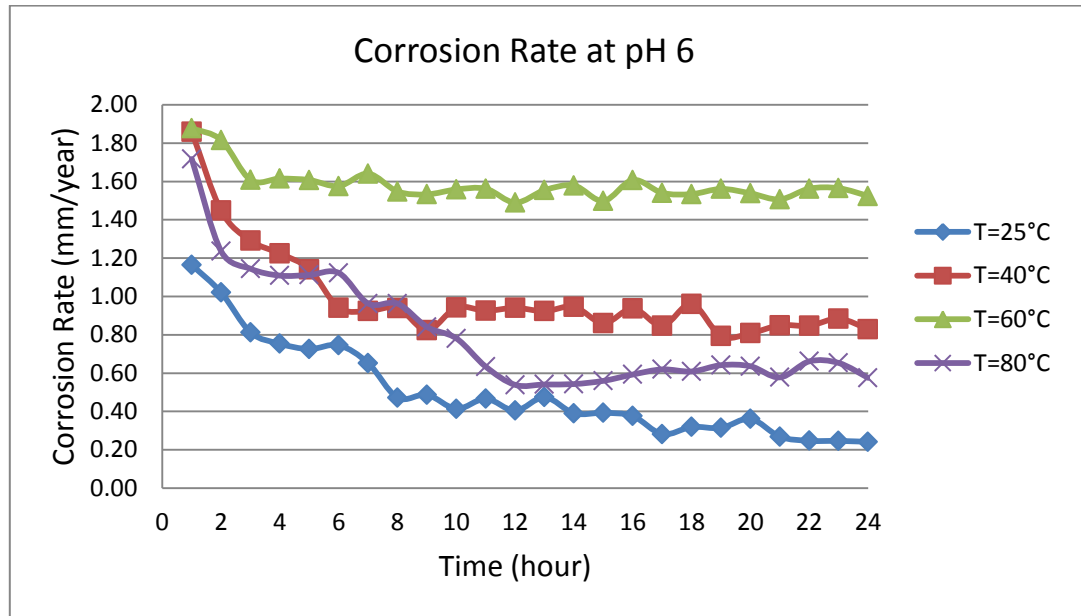


Figure 4.13: Corrosion rate at pH 6, recorded for 24 hours immersion of a carbon steel specimen in CO₂ saturated 3% NaCl solution with an addition of 50 ppm concentration of ions Fe²⁺ at various temperatures

Figure 4.13 shows the effect of temperatures to the corrosion rate at pH 6 for 24 hours immersion of a carbon steel specimen in CO₂ saturated 3% NaCl solution with an addition of 50 ppm concentration of ions Fe²⁺ at various temperatures of 25°C, 40°C, 60°C and 80°C. It shows that the trends of the corrosion rate are similar to the corrosion rate trends of natural film forming environment but with significant reduction in corrosion rate. This is due to the fact that the increase of concentration of ions Fe²⁺ from 0 ppm to 50 ppm, results in higher supersaturation,

which consequently accelerates the precipitation rate thus contribute to the formation of thicker FeCO_3 film layers.

It can be seen from Figure 4.14, that, after corrosion occurs for several hours, the corrosion rate started to decrease smoothly at eight (8) hours of experiment for all the temperatures. Besides, it also shows that at low temperatures (25°C , 40°C and 60°C), the corrosion rate increases as the temperature increases because of high solubility of the FeCO_3 film layers. However, at temperature of 80°C , the FeCO_3 film layers might have become more adherent to the steel surface and more protective in nature resulting in a decrease of the corrosion rate. This is because higher temperature increases kinetic of corrosion reaction, makes the solution saturated faster. Therefore, corrosion rate decreases significantly at temperature of 80°C which conforms that thicker FeCO_3 film layers form on the steel surface.

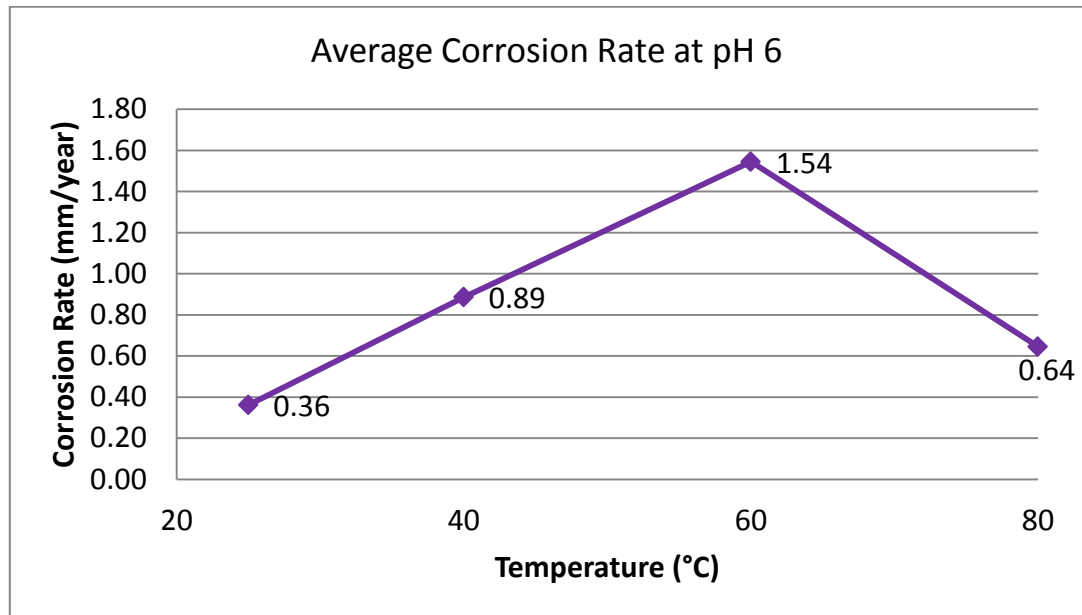
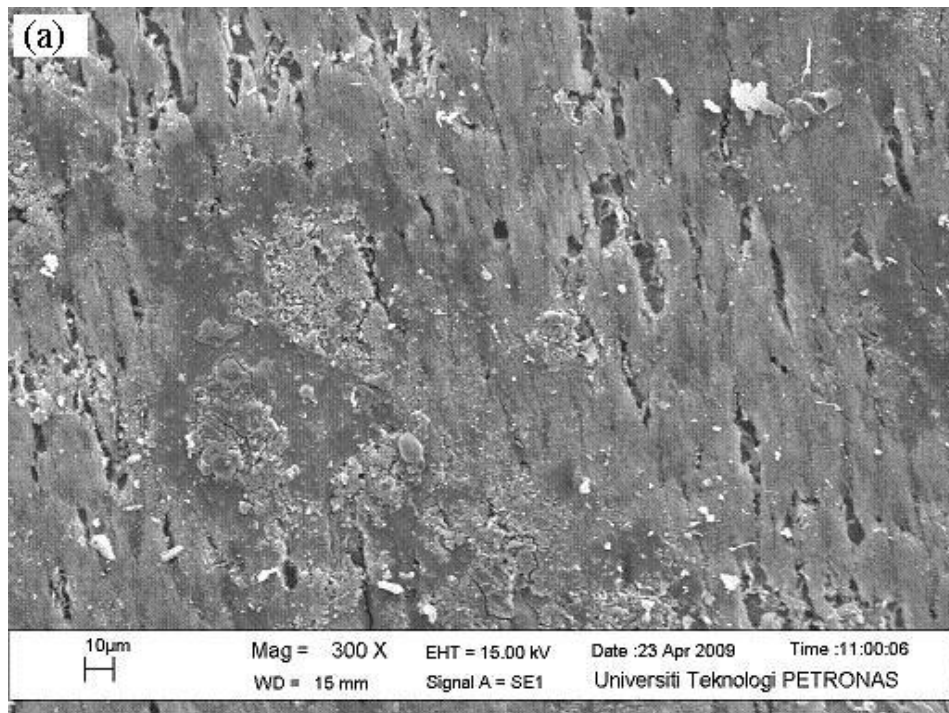


Figure 4.14: Average corrosion rate at pH 6 of a carbon steel specimen in CO_2 saturated 3% NaCl solution with an addition of 50 ppm concentration of ions Fe^{2+} at various temperatures

The average corrosion rate at pH 6 of a carbon steel specimen in CO_2 saturated 3% NaCl solution with an addition of 50 ppm concentration of ions Fe^{2+} for all

temperatures is then plotted together as shown in Figure 4.14 by taking the average value of the corrosion rate from eight (8) hours up to 24 hours of experiment for each experiment. This is done to observe the effect of temperature to the corrosion rate as it is known that increased temperature aids the formation of FeCO_3 film layers by accelerating the kinetics of precipitation. It is observed that the average corrosion rate of induced film forming environment shows similar trends to the average corrosion rate trends of natural film forming environment but with significant reduction in corrosion rate. From the results, it shows that the average corrosion rate at temperature of 25°C is the lowest with 0.36 mm/year which is then increases to 0.89 mm/year at temperature of 40°C . The highest corrosion rate is 1.54 mm/year at temperature of 60°C while at temperature of 80°C , the average corrosion rate decreases back to 0.64 mm/year where thick and dense FeCO_3 film layers might have been formed at the steel surface.

4.2.3 Scanning Electron Microscopy (SEM)



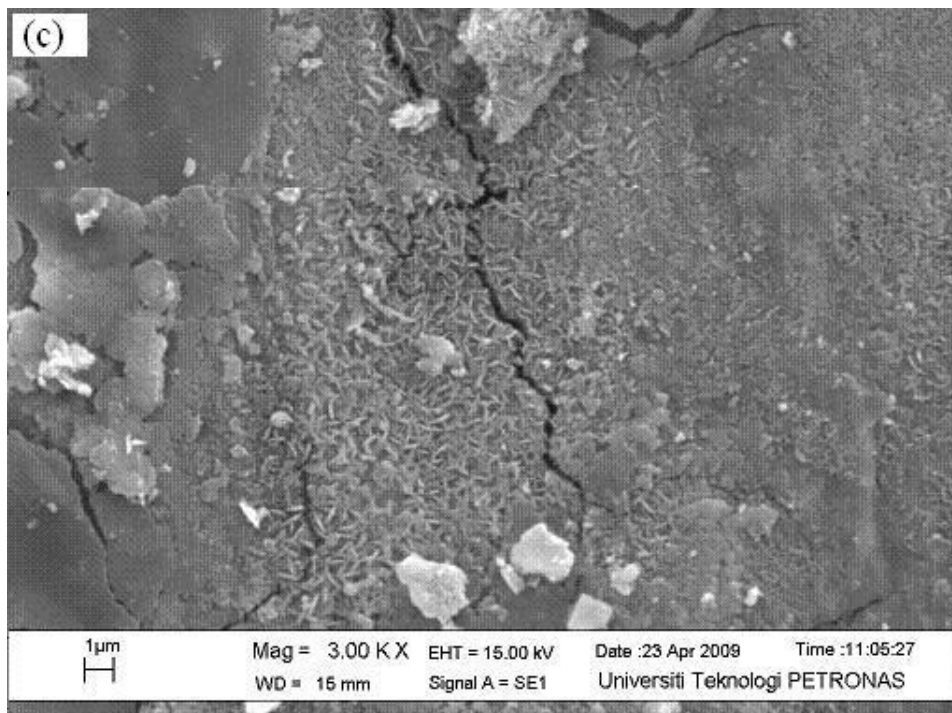
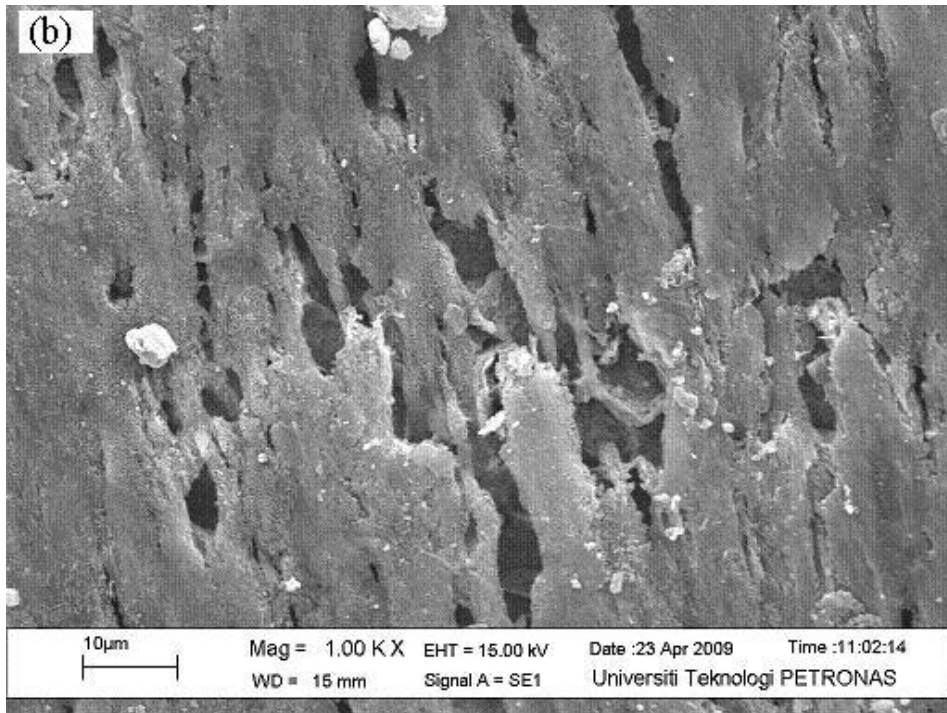


Figure 4.15: SEM images for 24 hours immersion of a carbon steel specimen in CO₂ saturated 3% NaCl solution with an addition of 50 ppm concentration of ions Fe²⁺ at temperature of 80°C (a) 300x (b) 1000x (c) 3000x

Figure 4.15 shows the SEM images of a carbon steel specimen in CO₂ saturated 3% NaCl solution with an addition of 50 ppm concentration of ions Fe²⁺ at temperature of 80°C in different magnification. It can be seen from the SEM images that the FeCO₃ film layers formed are still porous due to the fact that the experiments are only being done up to 24 hours. In fact, some cracks are also observed which conforms that the FeCO₃ film layers formed are still not protective. In order to form a very dense and protective FeCO₃ film layers, longer time of experiment is needed e.g. 48 – 96 hours.

4.3 Overall Corrosion Rate

Table 4.1: Average corrosion rate for natural film forming environment and induced film forming environment

Temperature (°C)	Average Corrosion Rate (mm/year)			
	Natural Film Forming Environment		Induced Film Forming Environment	
	EIS	LPR	EIS	LPR
25	1.53	1.54	0.67	0.36
40	2.78	2.01	1.86	0.89
60	3.56	2.69	2.73	1.54
80	4.36	1.93	3.08	0.64

Table 4.1 shows the tabulated data of overall corrosion rate using EIS and LPR techniques for natural film forming environment and induced film forming environment. It can be seen that, for natural film forming environment, using EIS technique, as the temperature increases from 25°C to 80°C, the average corrosion rate increases from 1.53 mm/year to 4.36 mm/year. In contrast, using LPR technique, the average corrosion rate increases from 1.54 mm/year at temperature of 25°C to 2.69 mm/year at 60°C before decreases to 1.93 mm/year at temperature of 80°C.

The average corrosion rate shows the same trend for induced film forming environment. It is shown in Table 4.1, for induced film forming environment, using EIS technique, as the temperature increases from 25°C to 80°C, the average corrosion rate increases from 0.67 mm/year to 3.08 mm/year. On the other hand, using LPR technique, the average corrosion rate increases from 0.36 mm/year at temperature of 25°C to 1.54 mm/year at 60°C before decreases to 0.64 mm/year at temperature of 80°C.

There are large differences between the average corrosion rate using EIS techniques as compared to LPR technique. This is because using EIS technique the average corrosion rate is calculated by taking the fitted values of polarization resistance, R_p from the semicircular diameter of the Nyquist plots. These values of R_p vary depending on how well the Nyquist plot is fitted. Besides, at temperature of 80°C, the fitted values of polarization resistance, R_p from the semicircular diameter are not taken the changes of shape of the Nyquist plot into account which explains the increases of the average corrosion rate. On the other hand, using LPR technique, the average corrosion rate is taken directly from the experimental data where at temperature of 80°C, the average corrosion decreases which conforms that thicker FeCO_3 film layers are already formed on the steel surface.

CHAPTER 5

CONCLUSION AND RECOMMENDATIONS

5.1 Conclusion

In corrosion rate measurement, for natural film forming environment, using EIS technique, as the temperature increases from 25°C to 80°C, the average corrosion rate increases from 1.53 mm/year to 4.36 mm/year. In contrast, using LPR technique, the average corrosion rate increases from 1.54 mm/year at temperature of 25°C to 2.69 mm/year at 60°C before decreases to 1.93 mm/year at temperature of 80°C.

For induced film forming environment, using EIS technique, as the temperature increases from 25°C to 80°C, the average corrosion rate increases from 0.67 mm/year to 3.08 mm/year. On the other hand, using LPR technique, the average corrosion rate increases from 0.36 mm/year at temperature of 25°C to 1.54 mm/year at 60°C before decreases to 0.64 mm/year at temperature of 80°C. It is observed that the average corrosion rate is relatively lower in induced film forming environment since the increase of Fe^{2+} concentration results in higher supersaturation, which consequently accelerates the precipitation rate and leads to higher surface scaling tendency and faster formation of FeCO_3 film layers which reduces the corrosion rate.

From the SEM images, for natural film forming environment, at temperature of 80°C, the FeCO_3 film layers are dense but still porous. Meanwhile, for induced film forming environment, at temperature of 80°C, the FeCO_3 film layers show some cracks. These characteristics explain the decreases of the average corrosion rate using LPR technique.

It is observed that the average corrosion rate is relatively lower in induced film forming environment since the increase of Fe^{2+} concentration results in faster formation of FeCO_3 film layers. Based on the results of the corrosion tests in both conditions, it shows that for corrosion prediction work, the test is best represented by natural film forming environment. Induced film condition is only suitable for the study in relations to film initiation, growth and propagation.

5.2 Recommendations

Further analysis can be done to improve the results of study. In determining the realistic results, comparison should be made between the experimental results and the calculation using CO_2 corrosion prediction models such as Cassandra and Norsok to verify the reliability and consistency of the results obtained from laboratory experiment.

Besides conducting experiment at temperatures of 25°C , 40°C , 60°C and 80°C , this study can be improved by including other temperatures which include temperatures of 50°C , 55°C , 70°C , 75°C , 85°C and 90°C . This is because under certain conditions, a difference of 5°C can lead to two different corrosion outcomes.

On the other hand, it was shown previously; both, experimentally and computationally that pH has a strong influence on the conditions leading to the formation of FeCO_3 film layers. Higher pH resulted in faster formation of more protective films and therefore, various pH such as pH 6.3 and pH 6.6 should be included in future work.

Parameters like flow velocity should be taken into consideration. This is because, prior to the formation of FeCO_3 film layers, high velocity increases corrosion rate as Fe^{2+} ions are transported away from the steel surface, leading to a lower concentration of Fe^{2+} ions at the steel surface thus contribute to less protective of FeCO_3 film formation.

Lastly, it is known that the presence of acetic acid (HAc) can have important effects on the CO₂ corrosion. Studies show that there is a great increase of the CO₂ corrosion rate in the presence of acetic acid at pH 4.0 while the effect vanished at pH 6.0 and higher. By including acetic acid in the study, the relationship between HAc and its role in the CO₂ corrosion, FeCO₃ film formation and its protectiveness to a steel surface can be determined.

REFERENCES

- [1] Kermani, M. B. and Smith, L. M. 1997. *CO₂ Corrosion Control in Oil and Gas Production – Design Consideration*. Number 23, London, The Institute of Materials.
- [2] Heuer, J.K. and Stubbins, J.F. 1998. *An XPS characterization on FeCO₃ films from CO₂ corrosion*. Corrosion Science 41 (1999) 1231-1243.
- [3] Jackman, P. S. and Smith, L. M. 1999. *Advances in Corrosion Control and Materials in Oil and Gas Production*. Number 26, London, The Institute of Materials.
- [4] Nestic, Srdjan, Lee, Kun-Lin John and Ruzic, Vukan. 2002. *A mechanistic model of iron carbonate film growth and the effect on CO₂ corrosion of carbon steel*. Corrosion 2002, Paper No. 02237, Houston, TX: NACE International, 2002.
- [5] van Hunnik, E.W.J., Pots, B.F.M and Hendriksen, E.L.J.A. 1996. *The formation of protective FeCO₃ corrosion product layers in CO₂ corrosion*. Corrosion 96, Paper No. 6, Houston, TX: NACE International, 1996.
- [6] Unknown Author <<http://www.ecochemie.nl/>>
- [7] ASTM Committee G01, 2004. *Standard Practice for Verification of Algorithm and Equipment for Electrochemical Impedance Measurements*. G 106 – 89 (Reapproved 2004), ASTM International, United States.

[8] Robert Baboian, 2005. *Corrosion Tests and Standards – Application and Intepretation*. 2nd Edition, ASTM International, United States.

[9] Unknown Author <<http://corrossion-doctors.org/Electrochem/EIS.htm>>

[10] S.L. Wu, Z.D. Cui, G.X. Zhao, M.L. Yan, S.L. Zhu and X.J. Yang. 2003. *EIS study of the surface film on the surface of carbon steel from supercritical carbon dioxide corrosion*. *Applied Surface Science* 228 (2004), Elsevier B.V., 2004.

APPENDIX: METHOD OF Fe²⁺ ADDITION

1. 100 mL of deionised water (DI water) was deoxygenated in a small beaker for about 15 minutes.
2. 1.78 g of FeCl₂·4H₂O was weighed in weighing dish.
3. FeCl₂ was added into the deoxygenated DI water.
4. After FeCl₂ was dissolved, the required amount of solution was removed out of the glass cell using a syringe and was added to the test solution by piercing the needle through the septum on the glass cell.
5. The amount of iron chloride solution added to the test solution to achieve a required concentration of Fe²⁺ (ppm), when 1.78 g of FeCl₂·4H₂O can be calculated using the following steps:
 - i. Molecular weight of Fe²⁺ = 56 g/mol
Molecular weight of FeCl₂·4H₂O = 198 g/mol
% of Fe²⁺ in FeCl₂·4H₂O = $\frac{56 \text{ g/mol}}{198 \text{ g/mol}} \times 100\%$
= 28.28 %
 - ii. To prepare solution with 5000 ppm or 0.5% of Fe²⁺, 1.78 g of FeCl₂·4H₂O was dissolved in 100 mL DI water
 - iii. The solution is further diluted by dissolved 1 mL of the solution in step (ii) with 100 mL DI water to achieve 50 ppm of Fe²⁺
6. The diluted solution containing 50 ppm of Fe²⁺ was always added before the metal sample was immersed in the test solution.